Chapter 3

Article 1

European Journal of Medicinal Chemistry

8-Aryl- and alkyloxycaffeine analogues as inhibitors of monoamine oxidase

Belinda Strydom[a], Jacobus J. Bergh[a], Jacobus P. Petzer[a]

[a]Pharmaceutical Chemistry, School of Pharmacy, North-West University, Private Bag X6001, Potchefstroom 2520, South Africa

European Journal of Medicinal Chemistry, 46 (2011) 3474–3485.

Graphical abstract:

The synthesis of 8-aryl- and alkyloxycaffeine analogues (**5**) with enhanced MAO-B inhibition potencies compared the lead compound, 8-benzyloxycaffeine (**2**).

		R	IC_{50} MAO-B (human) µM
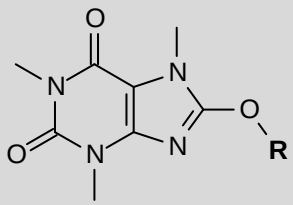	**2**	$C_6H_5CH_2$-	1.77
	5a	$C_6H_5(CH_2)_3$-	0.615
	5i	$C_6H_5OCH_2CH_2$-	0.383
	5k	$(CH_3)_2CH(CH_2)_4$-	0.381

8-Aryl- and alkyloxycaffeine analogues as inhibitors of monoamine oxidase

Belinda Strydom [a], Jacobus J. Bergh [a], Jacobus P. Petzer [a]

[a] *Pharmaceutical Chemistry, School of Pharmacy, North-West University, Private Bag X6001, Potchefstroom, 2520, South Africa*

Abstract—Recently it was reported that a series of 8-benzyloxycaffeine analogues are potent reversible inhibitors of human monoamine oxidase (MAO) A and B. In an attempt to discover additional C8 oxy substituents of caffeine that lead to potent MAO inhibition, a series of related 8-aryl- and alkyloxycaffeine analogues were synthesized and their MAO-A and –B inhibition potencies were compared to those of the 8-benzyloxycaffeines. The results document that while the 8-substituted-oxycaffeine analogues inhibited both human MAO isoforms, they displayed a high degree of selectivity for MAO-B. 8-(3-Phenylpropoxy)caffeine, 8-(2-phenoxyethoxy)caffeine and 8-[(5-methylhexyl)oxy]caffeine were found to be the especially potent MAO-B inhibitors with IC_{50} values ranging from 0.38–0.62 µM. These inhibitors are therefore 2.5–4.6 fold more potent MAO-B inhibitors than is 8-benzyloxycaffeine (IC_{50} = 1.77 µM). It is also demonstrated that, analogous to 8-benzyloxycaffeine, halogen substitution on the phenyl ring of the C8 substituent enhances MAO binding affinity by several orders of magnitude. For example, the most potent MAO-B inhibitor of the present series is 8-[2-(4-bromophenoxy)ethoxy]caffeine with an IC_{50} value of 0.166 µM. This study also reports possible binding orientations of selected oxycaffeines within the active site cavities of MAO-A and MAO-B.

Keywords: Monoamine oxidase; Reversible inhibition; 8-Aryloxycaffeine; 8-Alkyloxycaffeine; Caffeine; Molecular docking.

3.1 Introduction

The monoamine oxidases (MAO) A and B are mitochondrial bound flavin adenine dinucleotide (FAD) containing enzymes which catalyze the α-carbon oxidation of a variety of endogenous and dietary aminyl substrates in the brain and peripheral tissues [1,2]. The two MAO isoforms display different specificities towards substrates and inhibitors [3]. MAO-A catalyses the oxidation of serotonin and norepinephrine and is irreversibly inhibited by the mechanism-based inhibitor, clorgyline. MAO-B, on the other hand, catalyses the oxidation of benzylamine and is irreversibly inhibited by (*R*)-deprenyl. Both isoforms employ dopamine as substrate [3].

Because of their roles in the metabolism of neurotransmitter amines, MAO-A and –B are considered to be drug targets for the treatment of neuropsychiatric and neurodegenerative disorders. Inhibitors of MAO-A may elevate central serotonin levels and are therefore used in the treatment of depressive illness [4]. Moclobemide is an example of a selective MAO-A inhibitor that is currently being used as an antidepressant [5]. Since MAO-B is a major dopamine metabolizing enzyme in the basal ganglia of the primate brain, inhibitors of MAO-B are employed in the treatment of Parkinson's disease (PD) [6,7]. The inhibition of the MAO-B catalyzed metabolism of dopamine in the PD striatum may preserve the depleted dopamine supply [8] and elevate the levels of dopamine produced from exogenously administered levodopa [9,10]. For example, literature reports that MAO-B inhibitors enhance the elevation of dopamine levels in the striatum of primates treated with levodopa [9,10]. For these reasons, MAO-B inhibitors are frequently used as adjuvants to levodopa in the therapy of PD [6,11]. MAO-B inhibitors may also block the central production and accumulation of potentially neurotoxic species such as dopaldehyde and H_2O_2 which are formed during the MAO-B catalyzed metabolism of dopamine [12,13,14]. Based on this effect, MAO-B inhibitors are thought to protect against the neurodegenerative processes associated with PD [15]. This property of MAO-B inhibitors may be of particular relevance since the density and activity of MAO-B increases with age in most brain regions [16,17,18]. Examples of MAO-B inhibitors which are clinically used in PD therapy are (R)-deprenyl and rasagiline [19]. Both these drugs are selective for the MAO-B isoform and are propargylamine-containing mechanism-based inhibitors of the enzyme. Of interest is the observation that, even though MAO-

A activity is much lower than MAO-B activity in the striatum, both MAO-A and –B may contribute to catabolism of dopamine in the primate brain [20,18]. Literature reports that the extent by which the MAO-A selective inhibitor, clorgyline, enhances the elevation of dopamine levels in the striatum of primates treated with levodopa is similar to that obtained with (*R*)-deprenyl [9]. It has therefore been suggested that nonselective inhibitors of MAO may be more effective in the inhibition of dopamine catabolism and the treatment of PD [1].

While inactivators of MAO have been used extensively as clinical drugs, irreversible inhibition has a number of disadvantages [21]. These include the loss of isoform selectivity as a result of repeated drug administration and a slow and variable rate of enzyme recovery following withdrawal of the drug [22]. For example, the turnover rate for the biosynthesis of MAO-B in the human brain may require as much as 40 days [23]. In contrast, for reversible inhibition, enzyme activity is recovered when the inhibitor is eliminated from the tissues and the risk of loss of selectivity is reduced because of a shorter duration of action. Furthermore, where the mode of inhibition is competitive, the inhibition may be relieved when the substrate concentration is increased. Irreversible MAO-A inhibitors have the added disadvantage that it may potentiate the cardiovascular effects of indirectly acting sympathomimetic amines such as tyramine [1,4]. Inactivation of MAO-A in the gut wall greatly increases the quantity of tyramine entering the systemic circulation while reversible inhibition allows for the inhibitor to be displaced by tyramine which is subsequently normally metabolized by the enzyme. For these reasons several research groups are interested in the discovery of novel MAO inhibitors which interact reversibly with the enzymes.

For the design of reversible MAO inhibitors, a variety of scaffolds have been employed. Among these is caffeine (**1**) (Fig. 1). While caffeine (K_i = 3.6 mM) is a weak MAO-B inhibitor, literature reports that substitution of the caffeine ring at C8 with a variety of groups yields compounds endowed with greatly enhanced MAO-B inhibition activities than caffeine [24,25,26]. For example, a recent report documents that a series of 8-benzyloxycaffeine analogues act as potent reversible competitive inhibitors of both human MAO-A and –B [27]. In this series, 8-benzyloxycaffeine (**2**)

was found to inhibit MAO-B with an K_i value of 0.59 µM, approximately 6000 fold more potent than caffeine. 8-Benzyloxycaffeine also displayed affinity for MAO-A with an K_i value of 0.43 µM. Substitution on the benzyloxy ring with halogens enhances the MAO-A and –B inhibition potencies to an even greater extent. The benzyloxy side chain appears to be particularly effective in enhancing the binding affinities of reversible inhibitors for the active site of MAO-B. For example, both safinamide (**3**) and 7-(3-chlorobenzyloxy)-4-formylcoumarin (**4**) are potent MAO-B inhibitors and also contain halogen substituted-benzyloxy side chains (Fig. 1) [28]. The biological properties of the benzyloxy side chain with respect to its ability to bind to MAO-B may be best explained by considering the binding orientations of these inhibitors within the active site of MAO-B. The crystal structure of MAO-B in complex with safinamide show that the 3-fluorobenzyloxy side chain of safinamide extends into the entrance cavity of the MAO-B active site while the propanamidyl moiety binds within the substrate cavity [28]. In the crystal structure of MAO-B in complex with 7-(3-chlorobenzyloxy)-4-formylcoumarin, a similar binding orientation is observed with the 3-chlorobenzyloxy side chain located within the entrance cavity of the enzyme while the coumarin ring occupies the substrate cavity [28]. Modeling studies suggests that 8-benzyloxycaffeine may also bind to MAO-B with the caffeine moiety situated within the substrate cavity and the benzyloxy side chain extending towards the entrance cavity [27]. The interesting observation that 8-benzyloxycaffeines are also MAO-A inhibitors may possibly be attributed to the relatively large degree of rotational freedom of the benzyloxy side chain at the carbon-oxygen ether bond [27]. Previous studies have suggested that structures with a relatively larger degree of conformational freedom may be better suited for binding to MAO-A than relatively rigid structures [25].

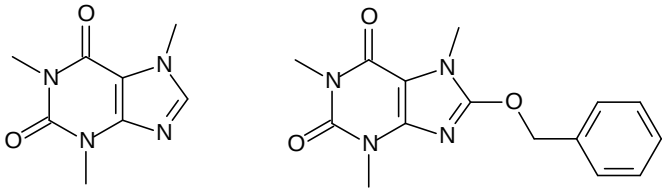

Caffeine (**1**)

8-Benzyloxycaffeine (**2**)

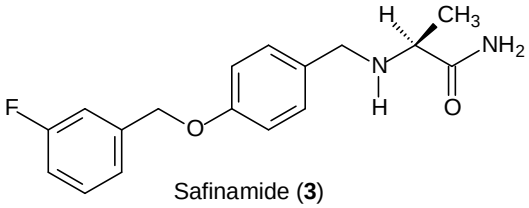

Safinamide (**3**)

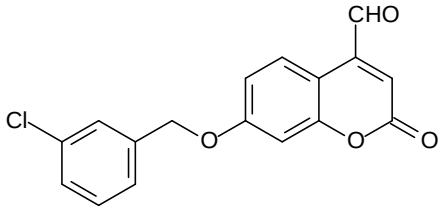

7-(3-Chlorobenzyloxy)-4-formylcoumarin (**4**)

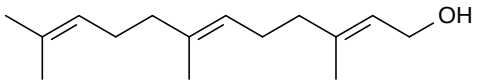

trans,trans-Farnesol (**7**)

Figure 1. The structures of known MAO inhibitors reported in this study.

In the present study, caffeine was substituted with a variety of C8 oxy substituents and the resulting analogues (**5a**–**n**) were evaluated as inhibitors of human MAO-A and –B (Table 1). The inhibition potencies of these analogues were compared to those of the previously reported 8-benzyloxycaffeines in an attempt to discover additional C8 oxy substituents of caffeine that lead to potent MAO inhibition [27]. For selected homologues, the effect of halogen substitution on the phenyl ring of the C8 substituent on MAO binding affinity was also investigated. As mentioned above, halogen substitution on the phenyl ring of 8-benzyloxycaffeine markedly enhances MAO inhibition potency [27]. In addition, in order to establish whether the test compounds bind reversibly with the MAO isozymes, the time-dependency of inhibition by selected analogues was investigated. As illustrated in Table 1, the oxy substituents that were selected for this study include phenyl, cycloalkane and cyclohexene rings attached via a variety of linkers at C8 of caffeine. In addition, two alkyloxy substituents (**5k**, **5l**) were also included. The most potent 8-aryloxycaffeine

(**5i**) identified in this study (see Results section) was further investigated by substitution with chlorine and bromine on the phenyl ring (**5m**, **5n**) and the measured MAO-A and –B inhibition potencies were compared to the corresponding halogen substituted 8-benzyloxycaffeienes (**5d**, **5e**).

Table 1: The structures of the C8 aryl- and alkyloxy substituted caffeine analogues (**5a**–**n**) that were synthesized and investigated in this study.

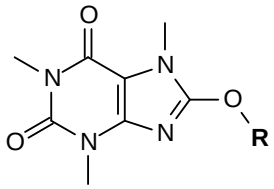

	-R		-R
5a	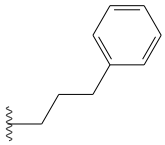	**5h**	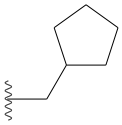
5b	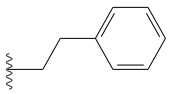	**5i**	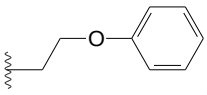
5c	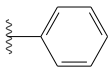	**5j**	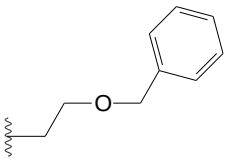
5d	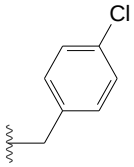	**5k**	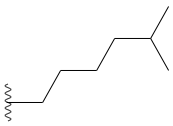
5e	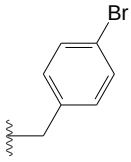	**5l**	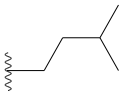
5f	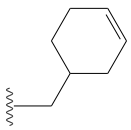	**5m**	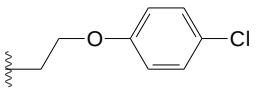
5g	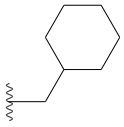	**5n**	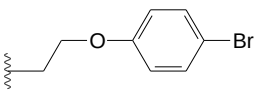

3.2. Results

3.2.1 Chemistry

The 8-aryl- and alkyloxycaffeine analogues (**5a**, **b**, **f**–**n**) that were investigated as potential MAO inhibitors were synthesized according to the general method previously described for the synthesis of C8 oxy substituted caffeine analogues [29,27]. As shown in Scheme 1 the target caffeine analogues were obtained by reacting 8-chlorocaffeine (**6**) with the appropriately substituted alcohol at high temperatures (150 ºC) in the presence of metallic sodium. After recrystallization from ethanol, the desired products (**5a**, **b**, **f**–**n**) were obtained in low to moderate yields of 7–40%. For the synthesis of 8-aryloxycaffeine analogues (**5c**–**e**) the reaction between the alcohol and 8-chlorocaffeine were carried out in the presence of potassium hydroxide [30]. 8-Chlorocaffeine was conveniently obtained in high yield by reacting chlorine with caffeine in chloroform [31]. The structures of all the compounds were verified by mass spectrometry, ^{1}H NMR and ^{13}C NMR while the purities were estimated by HPLC.

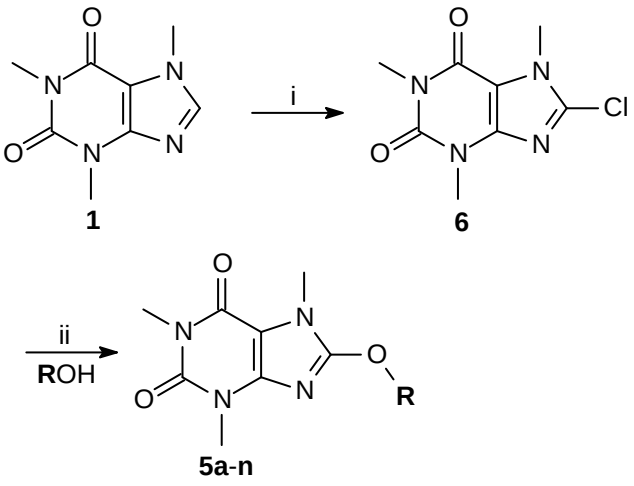

Scheme 1. Synthetic pathway to the C8 oxy substituted caffeine analogues **5a**–**n**. Reagents and conditions: (i) Cl_2, $CHCl_3$, (ii) Na or KOH, 150 ºC.

3.2.2 Enzymology

For the purpose of determining the MAO inhibition potencies of the study compounds, recombinant human MAO-A and –B were employed. The activities of both MAO isoforms were measured by using kynuramine as substrate [32]. Kynuramine, a mixed MAO-A/B substrate, is non-fluorescent and is oxidized by MAO to yield 4-hydroxyquinoline. The rates of MAO catalysis can be conveniently determined by measuring the formation of 4-hydroxyquinoline via fluorescence spectrophotometry at excitation and emission wavelengths of 310 nm and 400 nm, respectively. None of the inhibitors investigated in this study fluoresced at these excitation/emission wavelengths or quenched the fluorescence of 4-hydroxyquinoline at the inhibitor concentrations used. The experimentally determined IC_{50} values (Fig. 2) for the inhibition of the MAO isoforms were converted to the corresponding enzyme-inhibitor dissociation constants (K_i values) using the Cheng-Prusoff equation [33,26]. For this purpose K_m values for the oxidation of kynuramine by MAO-A and –B were used from previous studies. These are 16.1 µM for human MAO-A and 22.7 µM for human MAO-B [27]. These K_i values enabled the calculation of the MAO-A/B selectivity ratios [SI = K_i(MAO-B)/K_i(MAO-A)].

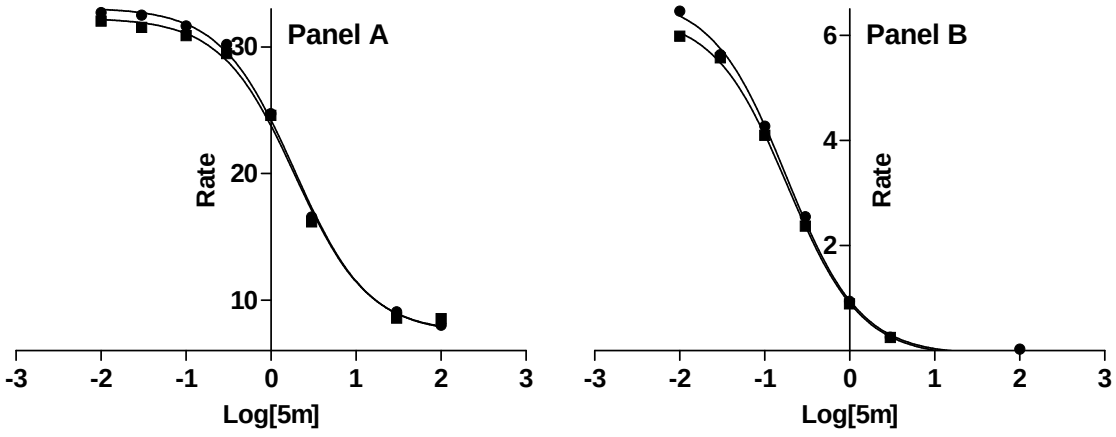

Figure 2. The recombinant human MAO-A (Panel A) and MAO-B (Panel B) catalyzed oxidation of kynuramine in the presence of various concentrations of inhibitor **5m**. The sigmoidal dose-response curves are constructed from the initial rates of oxidation of kynuramine (expressed as nmoles 4-hydroxyquinoline formed/min/mg protein) vs. the logarithm of concentration of inhibitor **5m** (expressed in nM). The concentrations of kynuramine used were 45 and 30 µM for the studies with MAO-A and MAO-B, respectively, and the determinations were carried out in duplicate and the values are expressed as the mean ± SD.

As shown in Table 2, all of the 8-aryl- and alkyloxycaffeine analogues (**5a**–**n**) were found to be inhibitors of both recombinant human MAO-A and –B. In general, the analogues exhibited relatively weak inhibition potencies towards MAO-A compared to MAO-B. In fact, with the exception of **5h** (SI = 1.46) which displayed a slight selectivity for MAO-A, all of the analogues evaluated were selective inhibitors of MAO-B (Table 2). Compound **5l** was essentially non-selective (SI = 1.08). Interestingly, the most potent MAO-A inhibitors were those containing halogen substitution on the phenyl ring of the C8 substituent. For example, the most potent MAO-A inhibitors of the present series are the halogen (chlorine and bromine) substituted homologues, **5d** and **5e**, with IC_{50} values of 1.34 µM and 1.30 µM, respectively. It can therefore be concluded that halogen substitution on the phenyl ring of the C8 substituent is a general strategy to enhance MAO-A binding affinity of caffeine derived inhibitors.

Table 2: The IC_{50} values for the inhibition of human MAO-A and –B by the C8 aryl- and alkyloxy substituted caffeine analogues **5a–n**.

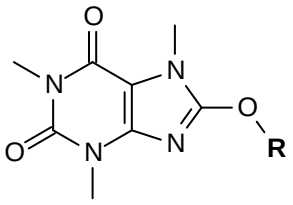

Compd.	**R**	IC_{50} MAO-A (human) µM	IC_{50} MAO-B (human) µM	K_i MAO-A (human) µM[a]	K_i MAO-B (human) µM[a]	SI[b]
5a	$C_6H_5(CH_2)_3$–	69.335 ± 1.69	0.615 ± 0.082	24.27	0.45	0.019
5b	$C_6H_5CH_2CH_2$–	15.925 ± 2.906	2.943 ± 0.281	5.57	2.16	0.39
5c	C_6H_5–	75.19 ± 7.849	10.705 ± 0.983	26.32	7.84	0.30
5d	4-$ClC_6H_4CH_2$–	1.337 ± 0.052	0.065 ± 0.001	0.47	0.048	0.10
5e	4-$BrC_6H_4CH_2$–	1.304 ± 0.034	0.062 ± 0.005	0.46	0.045	0.099
5f	$C_6H_9CH_2$–	13.755 ± 1.605	2.99 ± 0.17	4.81	2.19	0.45
5g	$C_6H_{11}CH_2$–	18.415 ± 3.175	1.365 ± 0.057	6.45	1.00	0.16
5h	$C_5H_9CH_2$–	22.81 ± 1.103	15.915 ± 3.401	7.98	11.65	1.46
5i	$C_6H_5OCH_2CH_2$–	20.35 ± 16.476	0.383 ± 0.021	77.12	0.28	0.0036
5j	$C_6H_5CH_2OCH_2CH_2$–	167.75 ± 13.223	3.772 ± 0.215	58.71	2.76	0.047
5k	$(CH_3)_2CH(CH_2)_4$–	15.17 ± 0.325	0.381 ± 0.082	5.31	0.28	0.053
5l	$(CH_3)_2CH(CH_2)_2$–	27.34 ± 2.079	14.13 ± 2.079	9.57	10.35	1.08
5m	4-$ClC_6H_4OCH_2CH_2$–	1.83 ± 0.013	0.183 ± 0.005	0.64	0.13	0.203
5n	4-$BrC_6H_4OCH_2CH_2$–	1.65 ± 0.087	0.166 ± 0.003	0.58	0.12	0.207

All values are expressed as the mean ± SD of duplicate determinations.

[a] The K_i values were calculated from the experimental IC_{50} values according to the equation by Cheng and Prusoff: $K_i = IC_{50}/(1 + [S]/K_m)$ with [S] = 30 µM and K_m (kynuramine) = 22.7 µM for human MAO-B while [S] = 45 µM and K_m (kynuramine) = 16.1 µM for human MAO-A [33].

[b] The selectivity index is the selectivity for the A isoform and is given as the ratio of K_i(MAO-B/K_i(MAO-A).

In contrast to their inhibition potencies towards MAO-A, the caffeine analogues **5a**–**n** were relatively potent MAO-B inhibitors. Among the most potent MAO-B inhibitors was the phenylpropoxy substituted caffeine analogue **5a** with an IC_{50} value of 0.615 µM. Interestingly, a reduction of the length of the substituent at C8 of caffeine is associated with a reduction of affinity for MAO-B. For example, both the benzyloxy (**2**) and phenylethoxy (**5b**) substituted caffeines are weaker MAO-B inhibitors than **5a** with IC_{50} values of 1.77 µM [27] and 2.94 µM, respectively. The 8-aryloxycaffeine analogue containing the shortest C8 substuituent, the phenoxy substituent, was particularly weak as a MAO-B inhibitor (IC_{50} = 10.7 µM). In agreement with these findings, the results also document that compound **5i**, with a C8 substituent (phenoxyethoxy) that is approximately equal in length to that of **5a**, is another potent MAO-B inhibitor with an IC_{50} value of 0.383 µM. A further increase in the length of the C8 substituent yields compounds with relatively lower MAO-B inhibition potencies. For example, **5j** with a benzyloxyethoxy side chain exhibits a reduction in MAO-B inhibition potency with an IC_{50} value of 3.77 µM, approximately 9 fold less potent than **5i**.

Replacement of the benzyloxy phenyl ring of **2** with cyclohexyl (**5f**), cyclohexenyl (**5g**) and cyclopentyl (**5h**) rings also yielded interesting results. Compared to **2** (IC_{50} = 1.77 µM) [27], the cyclohexylmethoxy substituent (**5g**) slightly improved MAO-B inhibition potency (IC_{50} = 1.37 µM) while the cyclohexenemethoxy substituent (**5f**) slightly reduced affinity for MAO-B (IC_{50} = 3.99 µM). The cyclopentylmethoxy substituent of caffeine **5h** was found to be the least favourable for MAO-B inhibition with **5h** being the weakest MAO-B inhibitor of the present series. These results indicate that replacement of the benzyloxy phenyl ring at C8 of caffeine with a cyclohexyl ring, may also lead to compounds endowed with potent MAO-B inhibitory properties. Also of note is the observation that compound **2** has a markedly lower IC_{50} value (IC_{50} = 1.24 µM) [27] for the inhibition of MAO-A than do compounds **5f**–**h**. This suggests that the phenyl ring is more optimal for MAO-A inhibition than the cyclohexyl (**5f**), cyclohexenyl (**5g**) and cyclopentyl (**5h**) rings.

Interestingly, the results also document that the branched-chain 8-alkyloxycaffeine analogues **5k** and **5l** are also MAO inhibitors. In fact, **5k** containing a 5-methylhexyloxy substituent at C8 of the caffeine ring proved to be a very potent and

selective MAO-B inhibitor with an IC_{50} value of 0.381 µM. Since the caffeine ring is thought to bind within the substrate cavity of MAO-B and the C8 side chain within the entrance cavity [27], this observation suggests that a ring system is not a requirement for interaction with the entrance cavity of the enzyme. This finding is in agreement with literature reports of the aliphatic alcohol, *trans*,*trans*-farnesol (**7**), acting as a selective MAO-B inhibitor (Fig. 1) [34]. *Trans*,*trans*-farnesol also exhibits a dual binding mode to the active site of MAO-B with the alcohol binding in close proximity to the FAD cofactor in the substrate cavity while the aliphatic chain extend towards the entrance cavity [34]. By employing docking studies, a possible binding mode and molecular interactions of **5k** within an MAO-B active site model will be proposed below.

In the present study, compounds **5m** and **5n**, the caffeine analogues containing halogens on the phenyl ring of the C8 substituent, were also found to be exceptionally potent inhibitors of MAO-B. These inhibitors, substituted with chlorine and bromine, exhibited IC_{50} values towards MAO-B of 0.183 µM and 0.166 µM, respectively. This result demonstrate that, analogous to the 8-benzyloxycaffeine studied previously [27], halogen substitution on the phenyl ring enhances MAO-B binding affinity by several orders of magnitude. The same result was obtained in the present study with 8-benzyloxycaffeines, **5d** and **5e**, exhibiting IC_{50} values of 0.065 µM and 0.062 µM, respectively. These compounds are approximately 27 fold more potent as MAO-B inhibitors than the parent unsubstituted 8-benzyloxycaffeine (**2**).

3.2.3 Reversibility studies

As discussed in the Introduction, reversible inhibition of MAO has certain advantages over irreversible inactivation of the MAO isozymes. One goal of this study is therefore to identify new oxycaffeine analogues that interact reversibly and with high affinity with MAO-A and/or –B. To investigate the reversibility of the interaction between the oxycaffeine analogues and MAO-A and –B, the time-dependence of inhibition by one representative inhibitor, compound **5n**, was evaluated. The selection of compound **5n** as representative inhibitor is based on the observation that it acts as a potent inhibitor of both MAO-A and –B. For this purpose, **5n** was preincubated with recombinant human MAO-A or-B for periods of 0, 15, 30 and 60 min and the residual rates by which MAO-A and –B catalyze the oxidation of kynuramine were measured.

The concentrations of **5n** that were selected for evaluating the time-dependence of inhibition of MAO-A and –B were 3.29 µM and 0.33 µM, respectively. These concentrations are approximately 2 fold the measured IC_{50} values for the inhibition of the respective enzymes by **5n**.

The results of the reversibility studies are shown in Fig. 3A and B. The graphs indicate that the rates of MAO-A and –B catalyzed oxidation of kynuramine do not decrease in a time-dependent manner when **5n** and the respective enzyme preparations are preincubated for various periods of time. These results demonstrate that **5n** interacts reversibly with both MAO-A and –B, at least at the inhibitor concentrations (2 × IC_{50}) and time period (60 min) used for these studies. This finding is in agreement with literature reports that the interactions between the MAO isozymes and C8 substituted caffeine are in general reversible [27,24,35,36].

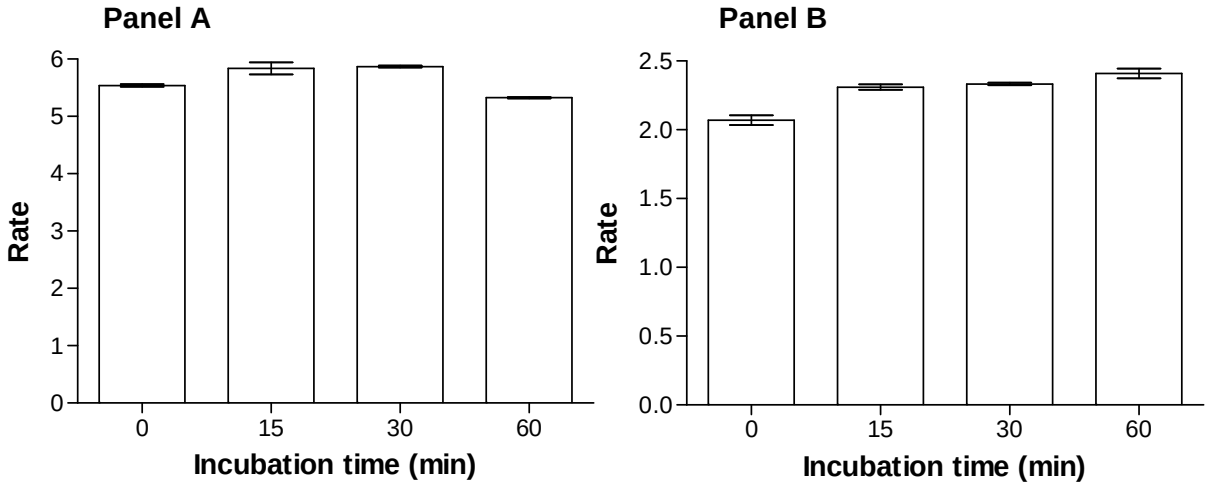

Figure 3. Time-dependence of the inhibition of the oxidation of kynuramine by recombinant human MAO-A (Panel A) and –B (Panel B). MAO-A and –B were preincubated for various periods of time (0–60 min) with **5n** at concentrations of 3.29 µM and 0.33 µM, respectively, and the residual catalytic rates were determined. The rates are expressed as nmoles 4-hydroxyquinoline formed/min/mg protein and the catalytic rates recorded in the absence of the inhibitors are 9.19 ± 0.31 and 6.38 ± 0.37 nmoles/min/mg for MAO-A and –B, respectively.

To provide further evidence for the reversibility of inhibition of MAO-A and –B by the oxycaffeine analogues examined in this study, sets of Lineweaver–Burk plots were constructed for the inhibition of both enzymes by **5n**, the selected representative inhibitor (Fig. 4A and B). Since the inhibition of both MAO-A and –B produce linear Lineweaver–Burk plots that intersect at the y-axis, it may be concluded that **5n** interacts competitively and, therefore, reversibly with both enzymes. From the replot of the slopes of the Lineweaver–Burk plots versus the inhibitor concentrations, K_i values of 1.18 µM and 0.088 µM were calculated for the inhibition of MAO-A and –B, respectively, by **5n**.

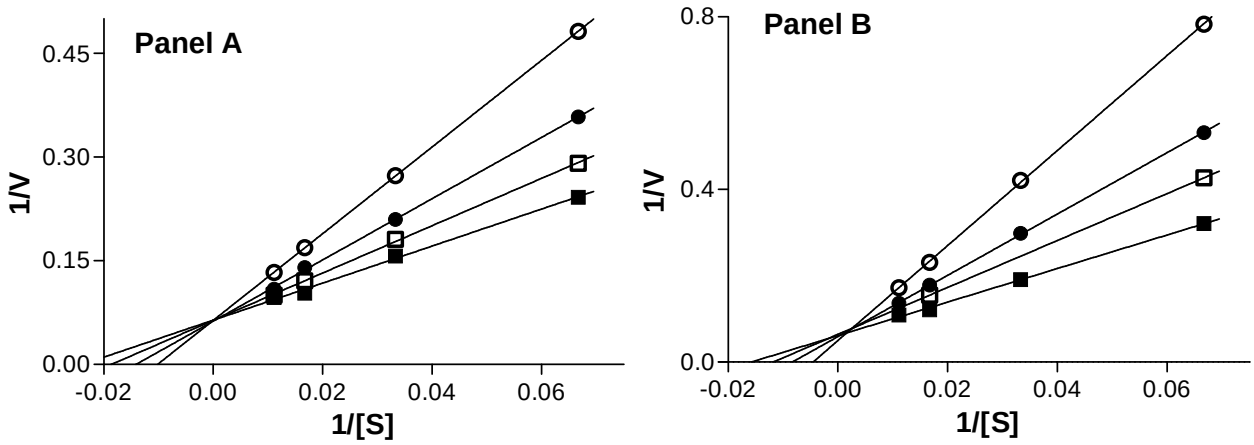

Figure 4. Lineweaver-Burk plots of the oxidation of kynuramine by recombinant human MAO-A (Panel A) and –B (Panel B) in the absence (filled squares) and presence of various concentrations of **5n**. For the studies with MAO-A (Panel A) the concentrations of **5n** were: 0.4125 µM (open squares), 0.825 µM (filled circles) and 1.65 µM (open circles). For the studies with MAO-B (Panel B) the concentrations of **5n** were: 0.0425 µM (open squares), 0.085 µM (filled circles) and 0.17 µM (open circles). The rates (V) are expressed as nmol product formed/min/mg protein.

3.2.4 Molecular modeling

The results of this study demonstrate that 8-aryl- and alkyloxycaffeine analogues (**5a**–**n**) are reversible inhibitors of both recombinant human MAO-A and –B and the analogues are in general selective for the MAO-B isoform. Interestingly, different oxy substituents at C8 of caffeine lead to relatively large differences in MAO inhibition potencies. For example the IC_{50} values for the inhibition of MAO-A ranged from 1.3–

167 µM while the IC_{50} values for the inhibition of MAO-B ranged from 0.062–15.9 µM. The MAO inhibition potencies appear to be dependent upon the length of the substituent at C8 of caffeine and the presence of halogens on the phenyl ring of the C8 substituent. To provide additional insight, the binding modes of selected 8-aryl- and alkyloxycaffeine analogues (**5a** and **5i**) in the active site cavities of MAO-A and –B were examined using molecular docking. These analogues were selected since they were found to be potent inhibitors of MAO-B.

For the purpose of the docking experiments, the crystallographic structures of human MAO-A in complex with harmine (PDB entry: 2Z5X) [37] and human MAO-B in complex with safinamide (PDB entry: 2V5Z) [28] were selected. These protein models were selected based on the high resolution of the crystallographic structures and the observation that, in the model of MAO-B, the side chain of Ile-199 occupies an alternate conformation which permits for the fusion of the substrate and entrance cavities. This is a requirement for the binding of relatively large inhibitors which extend from the substrate cavity into the entrance cavity [34]. The preparation of the protein models and the docking experiments were carried out according to a previously reported protocol with the Discovery Studio 1.7 modeling software [38,27]. After the valences of the FAD co-factor and the co-crystallised ligands were corrected, hydrogen atoms were added to the MAO-A and –B models and a three-step energy minimization procedure of the protein models was carried out (see Experimental). For this purpose, the backbones of the proteins were kept constrained. The co-crystallized ligands were subsequently extracted from the models and the binding cavities of the proteins were determined by the flood-filling algorithm. All crystal water molecules were removed except for those in the MAO-A and –B active sites that are considered conserved and non-displaceable (see Experimental). The structures of the ligands to be docked (**5a** and **5i**) were constructed and their geometries optimized within Discovery Studio and the ligands were docked into the active sites of the models with the LigandFit application within Discovery Studio. This protocol has been shown to be suitable for examining the binding of inhibitors to MAO-A and –B since redocking of harmine (RMSD = 0.64 Å) and safinamide (RMSD = 1.54 Å) into the active sites of the two enzymes, respectively, yielded binding orientations that exhibited relatively small RMSD values from the position of the co-crystallized ligands [39].

The predicted binding orientations of compounds **5a** and **5i** in the active site of MAO-B are shown in Fig. 5A–B. In all instances, the caffeine rings of the inhibitors bind within the substrate cavity of the enzyme, just in front of the flavin ring and approximately parallel to the phenolic side chains of the Tyr-398 and Tyr-435. This orientation is restricted by the flat shape of the substrate cavity of MAO-B [40]. Interestingly, the N1 methyl carbons of the caffeine rings of the inhibitors are positioned relatively closely to the FAD cofactor, approximately 3.6–4.1 Å from the flavin N5. This binding orientation brings the carbonyl oxygen at C6 of the caffeine ring within hydrogen bond interaction distance to an active site water molecule (HOH 1155) and the phenolic hydrogen of Tyr-435. A possible hydrogen bond interaction may also exist between the carbonyl oxygen at C2 of the caffeine ring and HOH 1346. Another productive interaction between the caffeine ring and the MAO-B active site is a possible π–π interactions with the amide functional group of the Gln-206 side chain with an interplane distance of approximately 3.5 Å may also exist [37]. These binding orientations and interactions are similar to those predicted by docking experiments previously for the binding of 8-benzyloxycaffeine (**2**) to MAO-B [27]. The results of the docking study also show that the C8 oxy substituents of caffeine extend towards the entrance cavity of the active site. The orientations of the C8 substituents of **5a** and **5i** within the entrance cavity are very similar. Since the entrance cavity is lined by the side chains of hydrophobic amino acid residues (Phe-103, Trp-119, Leu-164, Leu-167, Phe-168 and Ile-316), the C8 substituents are stabilized principally by Van der Waals interactions within the entrance cavity [32]. As discussed in the Introduction, the interaction of C8 substituted caffeine derivatives with both the substrate and entrance cavities of MAO-B may, for the most part, account for the potent MAO-B inhibition properties of compounds **5a**–**n** compared to caffeine.

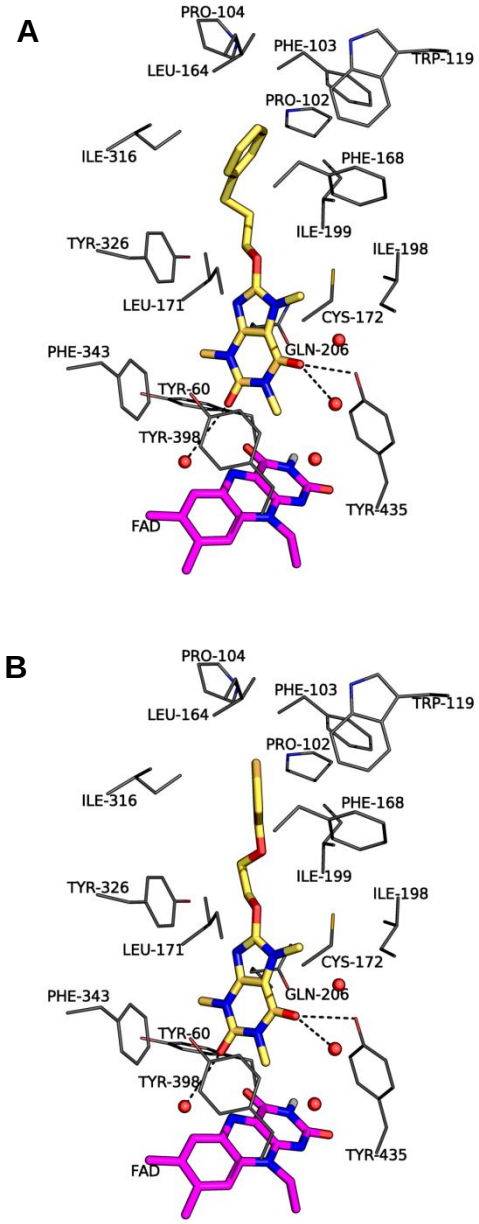

Figure 5. Predicted binding modes of **5a** (Panel A) and **5i** (Panel B) within the active site of MAO-B (2V5Z.pdb). The inhibitors are shown in yellow, the FAD cofactor in magenta and the active site amino acid residues in grey. These illustrations were generated with PyMol [45]

The predicted binding orientations of compound **5a** in the active site of MAO-A (Fig. 6) show that the caffeine rings adopt similar binding orientations to that observed in MAO-B, with the carbonyl oxygens at C2 of the caffeine rings located approximately 5.0–5.5 Å from the flavin N5. Only one potential hydrogen bond interaction between

the inhibitors and the MAO-A active site is observed – between the carbonyl oxygen at C2 of the caffeine ring and the phenolic hydrogen of Tyr-407. A possible π–π interaction between the amide functional group in the side chain of Gln-215 and the caffeine ring may represent another stabilizing factor (interplane distance, 3.5 Å) [37]. Similar to MAO-B, the C8 oxy substituent extends towards the entrance of the active site cavity. Also noteworthy is the observation that, in the MAO-A active site, the C8 oxy side chain of **5a** is bent by a larger extent from the plane of the caffeine ring compared the corresponding orientations that are adopted in the MAO-B active site (Fig. 7). A possible reason for this is that the caffeine rings bind comparatively distant from the FAD cofactor in the MAO-A active site than in the MAO-B active site. This reduces the space available for relatively long C8 side chains to bind within MAO-A and as a result, in order for the inhibitor to be accommodated within the active site, these side chains exist in a bent conformation relative to the plane of the caffeine ring.

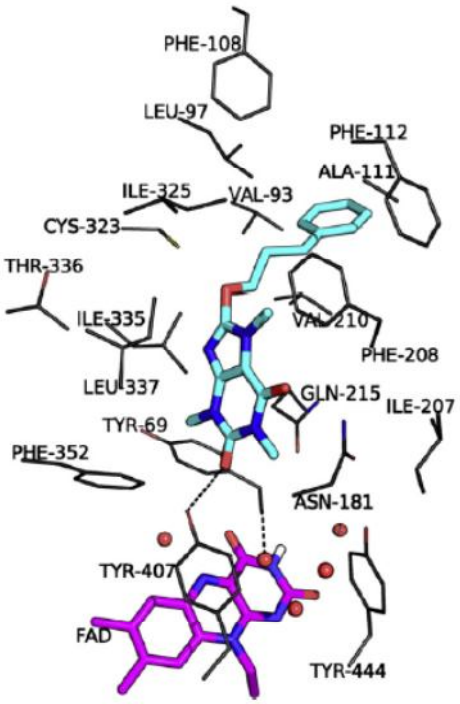

Figure 6. Predicted binding mode of **5a** within the active site of MAO-A (2Z5X.pdb). The inhibitor is shown in cyan, the FAD cofactor in magenta and the active site amino acid residues in grey. This illustration was generated with PyMol [45].

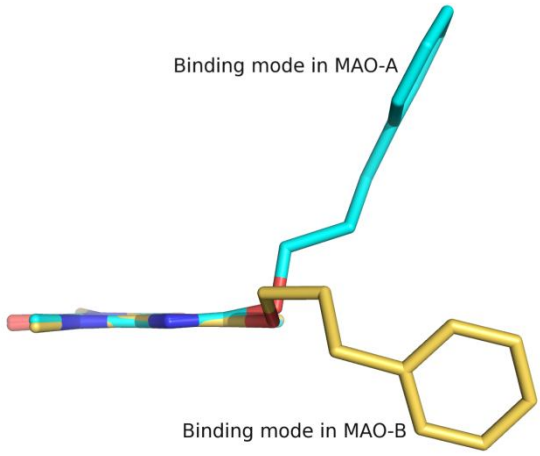

Figure 7. The predicted binding orientations of **5a** within the active sites of MAO-A (cyan) and MAO-B (yellow). This illustration was generated by superimposing the caffeine rings of the respective orientations.

3.3 Discussion

In the present study, a series of C8 oxy substituted caffeine analogues **5a**–**n** were synthesized and evaluated as inhibitors of recombinant human MAO-A and –B. The results demonstrate that, although the analogues inhibit both isozymes, they exhibit greater binding affinities for MAO-B. Molecular docking studies suggest that, in the MAO-B active site, the caffeine rings bind in closer proximity to the flavin cofactor compared to the binding orientation adopted in the MAO-A active site. This enables the caffeine ring to interact with MAO-B via 3 possible hydrogen bonds (2 to integral water molecules and 1 to Tyr-435) while only 1 hydrogen bond (with Tyr407) is formed between the caffeine ring and MAO-A. These observations may explain, in part, the MAO-B selective action of most of the oxy caffeines examined here. The C8 substituents may also play a role in determining the selectivity of caffeine analogues. For example, the previously studied 8-benzyloxycaffeine [27] exhibit little MAO-A/B selectivity. The molecular basis for this behavior, however, remains unclear. One possible reason may be that the relatively shorter C8 benzyloxy side chain may be better suited for binding to MAO-A than MAO-B. Also, by examining the interactions of one representative inhibitor (**5e**) with the enzymes it was concluded that the inhibition is reversible and competitive. This finding is in agreement with a previous report that 8-benzyloxyacaffeine analogues also are competitive reversible inhibitors of human MAO-A and –B [27].

Another interesting observation of the present study was the finding that among the aryloxy substituted caffeine analogues, compounds **5a** and **5i**, were particularly potent MAO-B inhibitors. The compounds contain phenylpropoxy and phenoxyethoxy C8 substituents, respectively, which are approximately equal in length. Analogues containing the shorter benzyloxy (**2**) [27] and phenylethoxy (**5b**) substituents as well as longer substituents such as the benzyloxyethoxy side chain (**5j**) proved to be weaker MAO-B inhibitors. These observations suggest that for the aryloxy substituted caffeienes, a linker consisting of 4 atoms separating the caffeine and the phenyl ring may be optimal for MAO-B inhibition. This linker length would allow for the best placement of the phenyl ring in the entrance cavity of the enzyme and hence the most productive interactions with the hydrophobic residues lining this space.

Caffeine analogues **5m** and **5n**, containing halogens on the phenyl ring of the C8 substituent, were also found to be remarkably potent inhibitors of MAO-B. Halogen substitution appears to be a general strategy to improve the inhibition potencies of a candidate MAO-A and –B inhibitors since substitution with halogens also enhances both the MAO-A and –B binding affinities of 8-benzyloxycaffeines as shown with compounds **5d** and **5e**. Literature reports that halogen substitution also enhances the MAO-B inhibition potencies of (E)-8-styrylcaffeienes [36] and (E)-2-styryl-1-methylbenzimidazoles [35]. A possible explanation may be that halogens may facilitate charge transfer or dipole interactions in the entrance cavity in addition to enhancing lipophilic interactions between the side chain and the hydrophobic environment of the entrance cavity [27]. In agreement with this view, literature reports that the MAO-B inhibition potencies of caffeinyl derived inhibitors frequently correlate with electronic properties as well as their lipophilicities of the substituents attached to the phenyl ring of the C8 side chain [27,36].

Interestingly, the caffeine analogues containing a cyclohexylmethoxy substituent (**5g**) was found to be slightly more potent as an MAO-B inhibitor than 8-benzyloxycaffeine (**2**) [27]. This indicates that the cyclohexyl and phenyl rings both form productive interactions with the entrance cavity of the enzyme that are approximately equal in strength. Substitution at C8 with side chains containing these two rings therefore enhances the MAO-B inhibition potency of caffeine to a similar extent. Another

noteworthy observation is the finding that the branched-chain 8-alkyloxycaffeine analogues **5k** act as a potent MAO-B inhibitor. Since the (methylhexyl)oxy side chain of **5k** would interact via hydrophobic burial with the residues of the entrance cavity, this finding demonstrates the importance of hydrophobic interactions between an inhibitor and the entrance cavity of MAO-B for the stabilization of the enzyme–inhibitor complex.

In conclusion, compounds **5a** and **5i**, which contain phenylpropoxy and phenoxyethoxy substituents at C8 of the caffeine ring may be viewed as promising lead compounds for the development of reversible MAO-B inhibitors. Both these compound exhibit improved MAO-B inhibition potencies compared to 8-benzyloxycaffeine which may be further improved via appropriate halogen substitution at the C8 substituent phenyl ring. This study demonstrates the importance of the length of the C8 side chain for the inhibition of MAO-B by caffeine analogues.

3.4. Experimental

3.4.1 Chemicals and instrumentation

All starting materials, unless noted elsewhere, were obtained from Sigma–Aldrich and were used without purification. Proton (^{1}H) and carbon (^{13}C) NMR spectra were recorded in $CDCl_3$ on a Bruker Avance III 600 spectrometer at frequencies of 600 MHz and 150 MHz, respectively. Chemical shifts are reported in parts per million (δ) downfield from the signal of tetramethylsilane added to the $CDCl_3$ (Merck). Spin multiplicities are given as s (singlet), d (doublet), t (triplet) or m (multiplet). Direct insertion electron impact ionization (EIMS) and high resolution mass spectra (HRMS) were obtained on a DFS high resolution magnetic sector mass spectrometer (Thermo Electron Corporation). Melting points (mp) were determined on a Stuart SMP10 melting point apparatus and are uncorrected. The purities of the synthesized compounds were estimated by HPLC analyses which were carried out with an Agilent 1100 HPLC system equipped with a quaternary pump and an Agilent 1100 series diode array detector (see Supplementary Material). For this purpose, HPLC grade acetonitrile (Merck) and Milli-Q water (Millipore) was used for the chromatography. Fluorescence spectrophotometry was conducted with a Varian Cary

Eclipse fluorescence spectrophotometer. Microsomes from insect cells containing recombinant MAO-A and –B (5 mg/mL) and kynuramine·2HBr that were required for the enzymatic reactions were obtained from Sigma–Aldrich. 8-Chlorocaffeine (**6**) was prepared according to a previously reported procedure [31] by reaction of caffeine with chlorine in chloroform. The melting point (188 ˚C) as well as the NMR data correlated to the corresponding published values [41,42].

*3.4.2 Procedures for the synthesis of the 8-aryl- and alkyloxycaffeine analogues (**5a–n**)*

For the synthesis of the target 8-aryl- and alkyloxycaffeine analogues **5a**, **b**, **f**–**n**, a method described in literature was followed with minor modifications [29]. Metallic sodium (1.5 mmol) and an appropriately substituted alcohol (21 mmol) were allowed to react with at room temperature. Following consumption of the sodium, 8-chlorocaffeine (**6**, 1.5 mmol) was added to the mixture and the resulting reaction was stirred for 6 hours at a temperature of 150 ˚C. The reaction was cooled to room temperature and the desired C8-substituted oxycaffeine analogues were recrystallized (at 4˚C) after the addition of ethanol (10–20 mL) to the reaction mixture.

For the synthesis of 8-aryloxycaffeine analogues (**5c**–**e**) the following literature method was followed [30]: Potassium hydroxide (2 mmol) was dissolved in 1 mL water and the appropriately substituted alcohol (1.85 mmol) was added to yield a solution. 8-Chlorocaffeine (**6**, 1.5 mmol) was added and the resulting reaction mixture was stirred at 150 ˚C for 6 hours. The reaction was cooled to room temperature and ethanol (10 mL) was added. The resulting precipitate was recrystallized (at 4˚C) from ethanol.

*3.4.2.1 8-(3-Phenylpropoxy)caffeine (**5a**)*

The title compound was prepared from 8-chlorocaffeine (**6**) and 3-phenylpropanol in a yield of 26%: mp 109 °C (ethanol). ^{1}H NMR (Bruker Avance III 600, $CDCl_3$) δ 2.18 (m, 2H), 2.81 (t, 2H, J = 7.5 Hz), 3.40 (s, 3H), 3.51 (s, 3H), 3.68 (s, 3H), 4.50 (t, 2H, J = 6.4 Hz), 7.23 (m, 3H), 7.31 (m, 2H); ^{13}C NMR (Bruker Avance III 600, $CDCl_3$) δ; 27.7, 29.7, 30.3, 32.0, 70.4, 103.4, 126.2, 128.4, 128.5, 140.8, 146.3, 151.7, 154.8, 155.7; EIMS 328.5; HRMS *m*/*z*: calcd for $C_{17}H_{20}N_4O_3$, 328.1535, found 328.1528; Purity (HPLC): 96.1%

*3.4.2.2 8-(3-Phenylethoxy)caffeine (**5b**)*

The title compound was prepared from 8-chlorocaffeine (**6**) and 2-phenylethanol in a yield of 40%: mp 144 °C (ethanol). ^{1}H NMR (Bruker Avance III 600, $CDCl_3$) δ 3.14 (t, 2H, J = 7.2 Hz), 3.39 (s, 3H), 3.52 (s, 3H), 3.66 (s, 3H), 4.68 (t, 2H, J = 7.2 Hz), 7.28 (m, 3H), 7.34 (m, 2H); ^{13}C NMR (Bruker Avance III 600, $CDCl_3$) δ; 27.7, 29.7, 35.4, 71.3, 103.4, 126.8, 128.61, 128.9, 137.1, 146.3, 151.7, 154.8, 155.3; EIMS 314.2; HRMS *m*/*z*: calcd for $C_{16}H_{18}N_4O_3$, 314.1379, found 314.13735; Purity (HPLC): 100%

*3.4.2.3 8-Phenoxycaffeine (**5c**)*

The title compound was prepared from 8-chlorocaffeine (**6**) and phenol in a yield of 24%: mp 140 °C (ethanol). ^{1}H NMR (Bruker Avance III 600, $CDCl_3$) δ 3.41 (s, 3H), 3.46 (s, 3H), 3.89 (s, 3H), 7.32 (m, 3H), 7.44 (m, 2H); ^{13}C NMR (Bruker Avance III 600, $CDCl_3$) δ; 27.8, 29.9, 30.4, 103.8, 119.4, 125.7, 129.8, 145.9, 151.6, 153.4, 153.5, 154.9; EIMS 286.1; HRMS *m*/*z*: calcd for $C_{14}H_{14}N_4O_3$, 286.1066, found286.10666; Purity (HPLC): 92.9%

*3.4.2.4 8-(4-Chlorobenzyloxy)caffeine (**5d**)*

The title compound was prepared from 8-chlorocaffeine (**6**) and 4-chlorobenzyl alcohol in a yield of 32%: mp 163 °C (ethanol). ^{1}H NMR (Bruker Avance III 600, $CDCl_3$) δ 3.39 (s, 3H), 3.54 (s, 3H), 3.71 (s, 3H), 5.46 (s, 2H), 7.40 (m, 4H); ^{13}C NMR (Bruker Avance III 600, $CDCl_3$) δ; 27.7, 29.7, 29.8, 71.7, 103.6, 129.0, 129.9, 133.5, 134.9, 146.1, 151.7, 154.8, 155.3; EIMS 334.1; HRMS *m*/*z*: calcd for $C_{15}H_{15}ClN_4O_3$, 334.0833, found 334.08329; Purity (HPLC): 96.9%

*3.4.2.5 8-(4-Bromobenzyloxy)caffeine (**5e**)*

The title compound was prepared from 8-chlorocaffeine (**6**) and 4-bromobenzyl alcohol in a yield of 17%: mp 179 °C (ethanol). ^{1}H NMR (Bruker Avance III 600, $CDCl_3$) δ 3.40 (s, 3H), 3.55 (s, 3H), 3.72 (s, 3H), 5.45 (s, 2H), 7.36 (d, 2H, J = 7.9 Hz), 7.56 (d, 2H, J = 7.9 Hz); ^{13}C NMR (Bruker Avance III 600, $CDCl_3$) δ; 27.8, 29.8, 29.9, 71.7, 103.6, 123.1, 130.1, 131.9, 134.0, 146.1, 151.7, 154.9, 155.3; EIMS 378.1; HRMS *m*/*z*: calcd for $C_{15}H_{15}BrN_4O_3$, 378.0328, found378.03387; Purity (HPLC): 96.3%

*3.4.2.6 8-(Cyclohex-3-en-1-ylmethoxy)caffeine (**5f**)*

The title compound was prepared from 8-chlorocaffeine (**6**) and 3-cyclohexen-1-ylmethanol in a yield of 18%: mp 170 °C (ethanol). ^{1}H NMR (Bruker Avance III 600, $CDCl_3$) *δ* 1.39 (m, 1H), 1.84 (m, 2H), 2.09 (m, 4H), 3.35 (s, 3H), 3.48 (s, 3H), 3.67 (s, 3H), 4.33 (d, 2H, J = 6.4 Hz), 5.68 (m, 2H); ^{13}C NMR (Bruker Avance III 600, $CDCl_3$) *δ*; 24.3, 25.0, 27.7, 27.8, 29.7, 33.3, 75.2, 103.3, 125.2, 127.1, 146.3, 151.7, 154.8, 155.9; EIMS 304.1; HRMS *m*/*z*: calcd for $C_{15}H_{20}N_4O_3$, 304.1535, found304.15385; Purity (HPLC): 96.9%

*3.4.2.7 8-Cyclohexylmethoxycaffeine (**5g**)*

The title compound was prepared from 8-chlorocaffeine (**6**) and cyclohexylmethanol in a yield of 24%: mp 120 °C (ethanol). ^{1}H NMR (Bruker Avance III 600, $CDCl_3$) *δ* 1.03 (m, 2H), 1.17 (m, 1H), 1.25 (m, 2H), 1.79 (m, 6H), 3.33 (s, 3H), 3.46 (s, 3H), 3.65 (s, 3H), 4.22 (d, 2H, J = 6.0 Hz); ^{13}C NMR (Bruker Avance III 600, $CDCl_3$) *δ*; 25.5, 26.3, 27.6, 29.4, 29.6, 29.7, 37.3, 76.1, 103.3, 146.3, 151.7, 154.7, 156.0; EIMS 306.2; HRMS *m*/*z*: calcd for $C_{15}H_{22}N_4O_3$, 306.1692, found 306.16901; Purity (HPLC):100%

*3.4.2.8 8-Cyclopentylmethoxycaffeine (**5h**)*

The title compound was prepared from 8-chlorocaffeine (**6**) and cyclopentylmethanol in a yield of 33%: mp 112 °C (ethanol). ^{1}H NMR (Bruker Avance III 600, $CDCl_3$) *δ* 1.33 (m, 2H), 1.61 (m, 4H), 1.79 (m, 2H), 2.36 (sept, 1H, J = 7.5 Hz), 3.36 (s, 3H), 3.48 (s, 3H), 3.66 (s, 3H), 4.31 (d, 2H, J = 7.2 Hz); ^{13}C NMR (Bruker Avance III 600, $CDCl_3$) *δ*; 25.3, 27.7, 29.1, 29.6, 29.7, 38.7, 74.9, 103.3, 146.3, 151.7, 154.8, 155.9; EIMS 292.2; HRMS *m*/*z*: calcd for $C_{14}H_{20}N_4O_3$, 292.1535, found 292.15378; Purity (HPLC): 100%

*3.4.2.9 8-(2-Phenoxyethoxy)caffeine (**5i**)*

The title compound was prepared from 8-chlorocaffeine (**6**) and 2-phenoxyethanol in a yield of 37%: mp 175 °C (ethanol). ^{1}H NMR (Bruker Avance III 600, $CDCl_3$) *δ* 3.36 (s, 3H), 3.48 (s, 3H), 3.66 (s, 3H), 4.32 (t, 2H, 4.9 Hz), 4.78 (t, 2H, 4.9 Hz), 6.91 (d, 2H, J = 7.5 Hz), 6.96 (t, 1H, J = 7.5 Hz), 7.28 (t, 2H, J = 7.5 Hz); ^{13}C NMR (Bruker Avance III 600, $CDCl_3$) *δ*; 27.7, 29.7, 29.8, 65.6, 69.3, 103.5, 114.6, 121.4, 129.5,

146.040, 151.6, 154.8, 155.3, 158.3; EIMS 330.2; HRMS *m*/*z*: calcd for $C_{16}H_{18}N_4O_4$, 330.1328, found 330.13232; Purity (HPLC): 94.9%

*3.4.2.10 8-[2-(Benzyloxy)ethoxy]caffeine (**5j**)*

The title compound was prepared from 8-chlorocaffeine (**6**) and 2-(benzyloxy)ethanol in a yield of 7%: mp 90 °C (ethanol). ^{1}H NMR (Bruker Avance III 600, $CDCl_3$) *δ* 3.36 (s, 3H), 3.47 (s, 3H), 3.68 (s, 3H), 3.81 (t, 2H, J = 4.5 Hz), 4.58 (s, 2H), 4.61 (t, 2H, J = 4.5 Hz), 7.27 (m, 1H), 7.32 (m, 4H); ^{13}C NMR (Bruker Avance III 600, $CDCl_3$) *δ*; 27.7, 29.7, 29.9, 67.7, 70.1, 73.2, 103.487, 127.7, 127.9, 128.5, 137.6, 146.1, 151.7, 154.8, 155.5; EIMS 344.1; HRMS *m*/*z*: calcd for $C_{17}H_{20}N_4O_4$, 344.1485, found 344.14822; Purity (HPLC): 94.7%

*3.4.2.11 8-[(5-Methylhexyl)oxy]caffeine (**5k**)*

The title compound was prepared from 8-chlorocaffeine (**6**) and 5-methyl-1-hexanol in a yield of 10%: mp 79 °C (ethanol). ^{1}H NMR (Bruker Avance III 600, $CDCl_3$) *δ* 0.87 (d, 6H, J = 6.8 Hz), 1.22 (m, 2H), 1.41 (m, 2H), 1.54 (sept, 1H, J = 6.8 Hz), 1.77 (quin, 2H, J = 7.5 Hz), 3.36 (s, 3H), 3.49 (s, 3H), 3.66 (s, 3H), 4.43 (t, 2H, J = 6.8 Hz); ^{13}C NMR (Bruker Avance III 600, $CDCl_3$) *δ*; 22.5, 23.4, 27.7, 27.8, 29.1, 29.7, 38.4, 71.2, 103.3, 146.4, 151.7, 154.8, 155.9; EIMS 308.2; HRMS *m*/*z*: calcd for $C_{15}H_{24}N_4O_3$, 308.1848, found 308.1855; Purity (HPLC): 100%

*3.4.2.12 8-(3-Methylbutoxy)caffeine (**5l**)*

The title compound was prepared from 8-chlorocaffeine (**6**) and 3-methyl-1-butanol in a yield of 37%: mp 130 °C (ethanol). ^{1}H NMR (Bruker Avance III 600, $CDCl_3$) *δ* 0.96 (d, 6H, J = 6.4 Hz), 1.68 (q, 2H, J = 6.8 Hz), 1.77 (sept, 1H, J = 6.8 Hz), 3.36 (s, 3H), 3.49 (s, 3H), 3.66 (s, 3H), 4.46 (t, 2H, J = 6.8 Hz); ^{13}C NMR (Bruker Avance III 600, $CDCl_3$) *δ*; 22.5, 24.9, 27.7, 29.7, 29.7, 37.6, 69.8, 103.3, 146.3, 151.7, 154.8, 155.9; EIMS 280.1; HROS *m*/*z*: calcd for $C_{13}H_{20}N_4O_3$, 280.1535, found 280.15366; Purity (HPLC): 100%

*3.4.2.13 8-[2-(4-Chlorophenoxy)ethoxy]caffeine (**5m**)*

The title compound was prepared from 8-chlorocaffeine (**6**) and 2-(4-chlorophenoxy)ethanol in a yield of 7.5%: mp 157 °C (ethanol). ^{1}H NMR (Bruker Avance IIK 600, $CDCl_3$) *δ* 3.35 (s, 3H), 3.48 (s, 3H), 3.66 (s, 3H), 4.29 (t, 2H, J = 4.52

Hz), 4.768 (t, 2H, J = 4.52), 6.83 (d, 2H, J = 9.04 Hz), 7.22 (d, 2H, J = 9.04 Hz); ^{13}C NMR (Bruker Avance III 600, $CDCl_3$) *δ*; 27.71, 29.70, 29.86, 66.05, 69.03, 103.57, 115.85, 126.28, 129.41, 146.00, 151.6, 154.76, 155.18, 156.89; Purity (HPLC): 92.14%

*3.4.2.14 8-[2-(4-Bromophenoxy)ethoxy]caffeine (**5n**)*

The title compound was prepared from 8-chlorocaffeine (**6**) and 2-(4-Bromophenoxy)ethanol in a yield of 9.9%: mp 165°C (ethanol). ^{1}H NMR (Bruker Avance III 600, $CDCl_3$) *δ* 3.35 (s, 3H), 3.48 (s, 3H), 3.67 (s, 3H), 4.286 (t, 2H, J = 4.52 Hz), 4.77 (t, 2H, J = 4.52 Hz), 6.79 (d, 2H, J = 9.04 Hz), 7.36 (d, 2H, J = 9.04 Hz); ^{13}C NMR (Bruker Avance III 600, $CDCl_3$) *δ*; 27.74, 29.73, 29.89, 65.99, 69.02, 103.61, 113.60, 116.38, 132.38, 146.03, 151.64, 154.80, 155.21, 157.42; EIMS 408.1; HRMS *m*/*z*: calcd for $C_{16}H_{17}BrN_4O_4$, 408.0433, found 408.04404; Purity (HPLC): 100%

3.4.3 IC_{50} determination for the inhibition of human MAO-A and –B

Microsomes from baculovirus infected insect cells expressing recombinant human MAO-A or –B (5 mg/mL) were obtained from Sigma-Aldrich and were pre-aliquoted and stored at –70 °C. All enzymatic reactions were carried out in 2 mL microcentrifuge tubes in potassium phosphate buffer (100 mM, pH 7.4) which were made isotonic with KCl (20.2 mM). The final volumes of the reactions were 500 µL and contained MAO-A or MAO-B (0.0075 mg/mL) and various concentrations of the test inhibitor (0–100 µM). Stock solutions of the test inhibitors were prepared in DMSO and added to the reactions to yield a final concentration of 4% (v/v) DMSO. Kynuramine served as enzyme substrate and were added to the reactions to yield final concentrations of 45 µM and 30 µM where MAO-A and –B, respectively, were used as enzymes. The reactions were incubated in a water bath at 37 °C for 20 min and terminated with the addition of 400 µL NaOH (2 N). Distilled water (1000 µL) was subsequently added to each reaction, and the concentrations of the MAO generated 4-hydroxyquinoline in the reactions were measured by fluorescence spectrophotometry ($\lambda_{excitation}$ = 310 nm, $\lambda_{emission}$ = 400 nm) [32]. For this purpose, a linear calibration curve was constructed from solutions of authentic 4-hydroxyquinoline (0.047–1.5 µM) dissolved in potassium phosphate buffer (100 mM, pH 7.4). To each standard 200 µL NaOH (2 N) and 1200 µL distilled water was

added. Sigmoidal dose–response curves were constructed by plotting the initial rates of kynuramine oxidation versus the logarithm of the inhibitor concentration. For each curve, 9 different inhibitor concentrations spanning at least 3 orders of a magnitude were used. To calculate the IC_{50} values, these data were fitted to the one site competition model incorporated into the Prism software package (GraphPad). All experiments were carried out duplicate and the IC_{50} values are expressed as mean ± standard deviation (SD) [27]. The IC_{50} values were converted to the corresponding K_i values according to the equation by Cheng and Prusoff: $K_i = IC_{50}/(1 + [S]/K_m)$ [33].

3.4.4. Time-dependence of inhibition

To determine whether the 8-aryl- and alkyloxycaffeine analogues act as reversible inhibitors or inactivators of MAO-A and –B, the time-dependence of inhibition were investigated over a period of 60 min. For this purpose, compound **5n** was selected as a representative inhibitor of the series. Compound **5n** was preincubated for periods of 0, 15, 30, 60 min at 37 ºC with recombinant human MAO-A or human MAO-B (0.03 mg/mL) in potassium phosphate buffer (100 mM, pH 7.4, made isotonic with KCl). The concentrations of **5n** employed for these reactions were 3.29 µM and 0.33 µM for the incubations with MAO-A and –B, respectively, and are approximately 2 fold the measured IC_{50} values for the inhibition of the respective MAO preparations. These preincubated enzyme preparations were then diluted 2 fold with the addition of kynuramine, at final concentrations of 45 µM and 30 µM for the reactions containing MAO-A and –B, respectively, and the resulting reactions were incubated at 37 °C for 15 minutes. The final volumes of these incubations were 500 µL, the final concentrations of the MAO preparations were 0.015 mg/mL and the final concentrations of **5n** were 1.65 µM and 0.165 µM for MAO-A and MAO-B, respectively. These concentrations of the inhibitor are approximately equal to the IC_{50} values for the inhibition of the respective enzyme preparations by **5n**. The reactions were terminated with 400 µL NaOH (2 N) and 1000 µL distilled water was added to each reaction. The rates of the MAO-catalyzed production of 4-hydroxyquinoline were measured as described above. All measurements were carried out in triplicate and are expressed as mean ± SD [43,44,27].

3.4.5. Mode of inhibition

To evaluate the mode of inhibition by the 8-aryl- and alkyloxycaffeine analogues, sets of Lineweaver–Burk plots for the inhibition of MAO-A and –B by compound **5n** were constructed. The initial rates of the MAO-catalyzed oxidation of kynuramine at four different substrate concentrations (15–90 µM) in the absence and presence of three different concentrations of **5n** were measured. The concentrations of **5n** that were selected ranged from 0.4125–1.65 µM and 0.0425–0.17 µM for the studies with MAO-A and –B, respectively. The enzymatic reactions and measurements were carried out as described above for the determination if the IC_{50} values. The only exception was that the concentrations of MAO-A and –B in the reactions were 0.015 mg/mL. Linear regression analysis was performed using the Prism software package [27].

3.4.6. Molecular modeling studies

Molecular docking of selected inhibitors (**5a** and **5i**) into the active sites of MAO-A and –B were carried out in the Windows based Discovery Studio 1.7 molecular modeling software [38]. The ligands to be docked were constructed Discovery Studio and the hydrogen atoms were added according to the appropriate protonation states at pH 7.4. Since flexible ligand docking were employed, their geometries required only brief optimization using a fast Dreiding-like forcefield (1000 iterations) in Discovery Studio. The atom potential types and partial charges were then automatically assigned with the Momany and Rone CHARMm forcefield. The X-ray crystallographic structures of MAO-A in complex with harmine (PDB code: 2Z5X) [37] and MAO-B in complex with safinamide (PDB code: 2V5Z) [28] were obtained from the Brookhaven Protein Data Bank (www.rcsb.org/pdb). Hydrogen atoms were added to the receptor models according to the appropriate protonation states of the ionizable amino acids at pH 7.4 and the valences of the FAD cofactors (oxidized state) and co-crystallized ligands were corrected and hydrogen atoms were added, also according to the appropriate protonation states at pH 7.4. The resulting models were automatically typed with the Momany and Rone CHARMm forcefield, the protein backbone was constrained and the models were subjected to a three step energy minimization cascade. The first step was a steepest descent minimization which was followed by conjugate gradient minimization. For both protocols the termination criteria was set to a maximum of 2500 steps or a minimum value of 0.1

for the root mean square of the energy gradient. The third step was an adopted basis Newton-Rapheson minimization with the termination criteria set to a maximum of 5000 steps or a minimum value for the root mean square of the energy gradient of 0.01. For this minimization cascade the implicit generalized Born solvation model with simple switching was used with the dielectric constant set to 4. The co-crystallized ligands were subsequently deleted from the active sites of the protein models, the backbone constraints were deleted and the binding site was identified by a flood-filling algorithm. The crystallized water molecules were removed with the exception of 4 active site water molecules. X-ray crystal structures of MAO-B have shown that only three active site water molecules (HOH 1155, 1170 and 1351; A-chain) are conserved, all in the vicinity of the FAD co-factor [28]. Preliminary docking studies in our laboratory suggest that HOH 1346 (MAO-B, A-chain) may also be involved in stabilizing caffeine analogues (by hydrogen bond interaction with carbonyl oxygen at C-6 of the caffeine ring) and were thus also retained. For the docking studies with MAO-A, the crystal waters were also deleted with the exception of HOH 710, 739 and 725 which occupies the analogous positions in the MAO-A active site to those positions that are occupied in the MAO-B active site by the waters cited above. HOH 726 which is located between the aromatic residues Tyr-407 and Tyr-444 was also retained since previous docking studies suggested that the caffeine do not bind in close proximity to this polar space [27]. Automated docking was subsequently carried out with the LigandFit application of Discovery Studio. This protocol uses total ligand flexibility whereby the final ligand conformations are determined by the Monte Carlo conformation search method set to a variable number of trial runs. The docked ligands were further refined using in situ ligand minimization with the Smart Minimizer algorithm. All parameters for the docking runs were set to their default values and ten possible binding solutions were computed for each docked ligand. The best-ranked binding conformation of each ligand was determined according to the DockScore values. The illustrations were prepared in PyMOL [45].

Acknowledgements

The NMR spectra were recorded by André Joubert of the SASOL Centre for Chemistry, North-West University while the MS spectra were recorded by Marelize Ferreira of the Mass Spectrometry Service, University of the Witwatersrand. This work was supported by grants from the National Research Foundation and the Medical Research Council, South Africa. The financial assistance of the National Research Foundation (DAAD-NRF) towards this research is hereby acknowledged. Opinions expressed and conclusions arrived at, are those of the authors and are not necessarily to be attributed to the DAAD-NRF.

References

[1] M.B.H. Youdim, Y.S. Bakhle, Monoamine oxidase: Isoforms and inhibitors in Parkinson's disease and depressive illness, Br. J. Pharmacol. 147 (2006) S287.

[2] C. Binda, P. Newton-Vinson, F. Hubalek, D.E. Edmondson, A. Mattevi, Structure of human monoamine oxidase B, a drug target for the treatment of neurological disorders, Nature Struct. Biol. 9 (2002) 22-26.

[3] M.B.H. Youdim, D.E. Edmondson, K.F. Tipton, The therapeutic potential of monoamine oxidase inhibitors, Nat. Rev. Neurosci. 7 (2006) 295-309.

[4] M.B.H. Youdim, M. Weinstock, Therapeutic Applications of Selective and Non-Selective Inhibitors of Monoamine Oxidase A and B that do not Cause Significant Tyramine Potentiation, Neurotoxicology. 25 (2004) 243-250.

[5] U. Bonnet, Moclobemide: therapeutic use and clinical studies, CNS. Drug. Rev. 9 (2003) 97-140.

[6] H.H. Fernandez, J.J. Chen, Monoamine oxidase-B inhibition in the treatment of Parkinson's disease, Pharmacotherapy. 27 (2007) 174S.

[7] G.G.S. Collins, M. Sandler, E.D. Williams, M.B.H. Youdim, Multiple forms of human brain monoamine oxidase, Nature. 225 (1970) 817-820.

[8] P. Riederer, M.B.H. Youdim, Monoamine oxidase activity and monoamine metabolism in brains of parkinsonian patients treated with l-deprenyl, J. Neurochem. 46 (1986) 1359-1365.

[9] D.A. Di Monte, L.E. DeLanney, I. Irwin, J.E. Royland, P. Chan, M.W. Jacowec, J.W. Langston, Monoamine oxidase-dependent metabolism of dopamine in the striatum and substantia nigra of L-DOPA-treated monkeys, Brain Res. 738 (1996) 53-59.

[10] J.P. Finberg, J. Wang, K. Bankiewich, J. Harvey-White, I.J. Kopin, D.S. Goldstein, Increased striatal dopamine production from L-DOPA following selective inhibition of monoamine oxidase B by R(+)-*N*-propargyl-1-aminoindan (rasagiline) in the monkey, J. Neural Transm. Suppl. 52 (1998) 279.

[11] W. Birkmayer, P. Riederer, M.B.H. Youdim, W. Linaur, The potentiation of the anti-akinetic effect after L-dopa treatment by an inhibitor of MAO-B, L-deprenyl, J. Neural. Transm. 36 (1975) 303-326.

[12] M. Gesi, A. Santinami, R. Ruffoli, G. Conti, F. Fornai, Novel Aspects of Dopamine Oxidative Metabolism (Confounding Outcomes Take Place of Certainties, Pharmacol. Toxicol. 89 (2001) 217-224.

[13] F. Fornai, G. Battaglia, M. Gesi, F.S. Giorgi, F. Orzi, F. Nicoletti, Time-course and dose-response study on the effects of chronic L-DOPA administration on striatal dopamine levels and dopamine transporter following MPTP toxicity, Brain Res. 887 (2000) 110-117.

[14] S.A. Marchitti, R.A. Deitrich, V. Vasiliou, Neurotoxicity and metabolism of the catecholamine-derived 3,4-dihydroxyphenylacetaldehyde and 3,4-dihydroxyphenylglycolaldehyde: The role of aldehyde dehydrogenase, Pharmacol. Rev. 59 (2007) 125-150.

[15] J.P. Petzer, N. Castagnoli Jr., M.A. Schwarzschild, J. Chen, C.J. Van der Schyf, Dual-target-directed drugs that block monoamine oxidase B and

adenosine A_{2A} receptors for parkinson's disease, Neurotherapeutics. 6 (2009) 141-151.

[16] A. Nicotra, F. Pierucci, H. Parvez, O. Santori, Monoamine oxidase expression during development and aging, Neurotoxicology. 25 (2004) 155.

[17] J.S. Fowler, N.D. Volkow, G.J. Wang, J. Logan, N. Pappas, C. Shea, R. MacGregor, Age-related increases in brain monoamine oxidase B in living healthy human subjects, Neurobiol. Aging. 18 (1997) 431-435.

[18] R.N. Kalaria, M.J. Mitchell, S.I. Harik, Monoamine oxidases of the human brain and liver, Brain. 111 (1988) 1441-1451.

[19] J.M. Rabey, I. Sagi, M. Huberman, E. Melamed, A. Korczyn, N. Giladi, R. Inzelberg, R. Djaldetti, C. Klein, G. Berecz, Rasagiline mesylate, a new MAO-B inhibitor for the treatment of parkinson's disease: A double-blind study as adjunctive therapy to levodopa, Clin. Neuropharmacol. 23 (2000) 324-330.

[20] C.J. Fowler, A. Wiberg, L. Oreland, B. Winblad, Titration of human brain type-B monoamine oxidase, Neurochem. Res. 5 (1980) 697-708.

[21] L.H.A. Prins, J.P. Petzer, S.F. Malan, Inhibition of monoamine oxidase by indole and benzofuran derivatives, Eur. J. Med. Chem. 45 (2010) 4458-4466.

[22] K.F. Tipton, S. Boyce, J. O'Sullivan, G.P. Davey, J. Healy, Monoamine oxidases: Certainties and uncertainties, Curr. Med. Chem. 11 (2004) 1965-1982.

[23] J.S. Fowler, N.D. Volkow, J. Logan, G. Wang, R.R. MacGregor, D. Schlyer, A.P. Wolf, N. Pappas, D. Alexoff, C. Shea, E. Dorflinger, L. Kruchowy, K. Yoo, E. Fazzini, C. Patlak, Slow recovery of human brain MAO B after L-deprenyl (selegeline) withdrawal, Synaps. 18 (1994) 86-93.

[24] J.P. Petzer, S. Steyn, K.P. Castagnoli, J. Chen, M.A. Schwarzchild, C.J. Van Der Schyf, N. Castagnoli, Inhibition of monoamine oxidase B by selective adenosine A_{2A} receptor antagonists, Bioorg. Med. Chem. 11 (2003) 1299-1310.

[25] E.M. Van der Walt, E.M. Milczek, S.F. Malan, D.E. Edmondson, N. Castagnoli, J.J. Bergh, J.P. Petzer, Inhibition of monoamine oxidase by (E)-styrylisatin analogues, Bioorg. Med. Chem. Lett. 19 (2009) 2509-2513.

[26] J. Pretorius, S.F. Malan, N. Castagnoli, J.J. Bergh, J.P. Petzer, Dual inhibition of monoamine oxidase B and antagonism of the adenosine A_{2A} receptor by (E,E)-8-(4-phenylbutadien-1-yl)caffeine analogues, Bioorg. Med. Chem. 16 (2008) 8676-8684.

[27] B. Strydom, S.F. Malan, N. Castagnoli, J.J. Bergh, J.P. Petzer, Inhibition of monoamine oxidase by 8-benzyloxycaffeine analogues, Bioorg. Med. Chem. 18 (2010) 1018-1028.

[28] C. Binda, J. Wang, L. Pisani, C. Caccia, A. Carotti, P. Salvati, D.E. Edmondson, A. Mattevi, Structures of human monoamine oxidase B complexes with selective noncovalent inhibitors: Safinamide and coumarin analogs, J. Med. Chem. 50 (2007) 5848-5852.

[29] R.C. Huston, W.F. Allen, Caffeine derivatives. I. The 8-ethers of caffeine, 56 (1934) 1356-1358.

[30] W. Baumann, Die nervenkrankenfürsorge der stadt essen, Z. Gesamte Neurol. Psychiatr. 15 (1913) 114-121.

[31] E. Fischer, L. Reese, Ueber Caffeïn, Xanthin und Guanin, Justus Liebigs Ann. Chem. 221 (1883) 336-344.

[32] L. Novaroli, M. Reist, E. Favre, A. Carotti, M. Catto, P.A. Carrupt, Human recombinant monoamine oxidase B as reliable and efficient enzyme source for inhibitor screening, Bioorg. Med. Chem. 13 (2005) 6212-6217.

[33] Y.C. Cheng, W.H. Prusoff, Relationship between the inhibition constant (K1) and the concentration of inhibitor which causes 50 per cent inhibition (I50) of an enzymatic reaction, Biochem. Pharmacol. 22 (1973) 3099-3108.

[34] F. Hubálek, C. Binda, A. Khalil, M. Li, A. Mattevi, N. Castagnoli, D.E. Edmondson, Demonstration of isoleucine 199 as a structural determinant for

the selective inhibition of human monoamine oxidase B by specific reversible inhibitors, J. Biol. Chem. 280 (2005) 15761-15766.

[35] D. Van den Berg, K.R. Zoellner, M.O. Ogunrombi, S.F. Malan, G. Terre'Blanche, N. Castagnoli, J.J. Bergh, J.P. Petzer, Inhibition of monoamine oxidase B by selected benzimidazole and caffeine analogues, Bioorg. Med. Chem. 15 (2007) 3692-3702.

[36] N. Vlok, S.F. Malan, N. Castagnoli, J.J. Bergh, J.P. Petzer, Inhibition of monoamine oxidase B by analogues of the adenosine A2A receptor antagonist (E)-8-(3-chlorostyryl)caffeine (CSC), Bioorg. Med. Chem. 14 (2006) 3512-3521.

[37] S.-Y. Son, J. Ma, Y. Kondou, M. Yoshimura, E. Yamashita, T. Tsukihara, Structure of human monoamine oxidase A at 2.2-A resolution: the control of opening the entry for substrates/inhibitors, Proc. Natl. Acad. Sci. U.S.A. 105 (2008) 5739-5744.

[38] Accelrys Discovery Studio 1.7, Accelrys Software Inc., San Diego, CA, USA. 2006, http://www.accelrys.com.

[39] C.I. Manley-King, J.J. Bergh, J.P. Petzer, Inhibition of monoamine oxidase by selected C5- and C6-substituted isatin analogues Bioorg. Med. Chem. 19 (2011) 261-274.

[40] C. Binda, R. Angelini, R. Federico, P. Ascenzi, A. Mattevi, Structural bases for inhibitor binding and catalysis in polyamine oxidase, Biochemistry. 40 (2001) 2766-2776.

[41] E. Fischer, Ueber Caffeïn, Theobromin, Xanthin und Guanin, Justus Liebigs Ann. Chem. 215 (1882) 267.

[42] M. Sono, N. Toyoda, K. Shimizu, E. Noda, Y. Shizuri, M. Tori, Functionalization including fluorination of nitrogen-containing compounds using electrochemical oxidation, Chem. Pharm. Bull. 44 (1996) 1141-1145.

[43] M.O. Ogunrombi, S.F. Malan, G. Terre'Blanche, N. Castagnoli, J.J Bergh, J.P. Petzer, Structure-activity relationships in the inhibition of monoamine oxidase B by 1-methyl-3-phenylpyrroles, Bioorg. Med. Chem. 16 (2008) 2463-2472.

[44] C.I. Manley-King, G. Terre'Blanche, N. Castagnoli, J.J. Bergh, J.P. Petzer, Inhibition of monoamine oxidase B by N-methyl-2-phenylmaleimides, Bioorg. Med. Chem. 17 (2009) 3104-3110.

[45] W.L. DeLano, Palo Alto, CA, USA. 2002.

Supplementary Material

S1: HPLC traces of the following new/unknown compounds

Method: To determine the purity of compounds **5a**–**n**, HPLC analyses were carried out. HPLC analyses were performed with an Agilent 1100 HPLC system equipped with a quaternary pump and an Agilent 1100 series diode array detector. A Venusil XBP C18 column (4.60 × 150 mm, 5 µm) was used and the mobile phase consisted initially of 30% acetonitrile and 70% MilliQ water at a flow rate of 1 mL/min. At the start of each HPLC run a solvent gradient program was initiated by linearly increasing the composition of the acetonitrile in the mobile phase to 85% acetonitrile over a period of 5 min. Each HPLC run lasted 15 min and a time period of 5 min was allowed for equilibration between runs. A volume of 20 µL of solutions of the test compounds in acetonitrile (1 mM) was injected into the HPLC system and the eluent was monitored at wavelengths of 210, 254 and 300 nm.

8-(3-Phenylpropoxy)caffeine (5a)

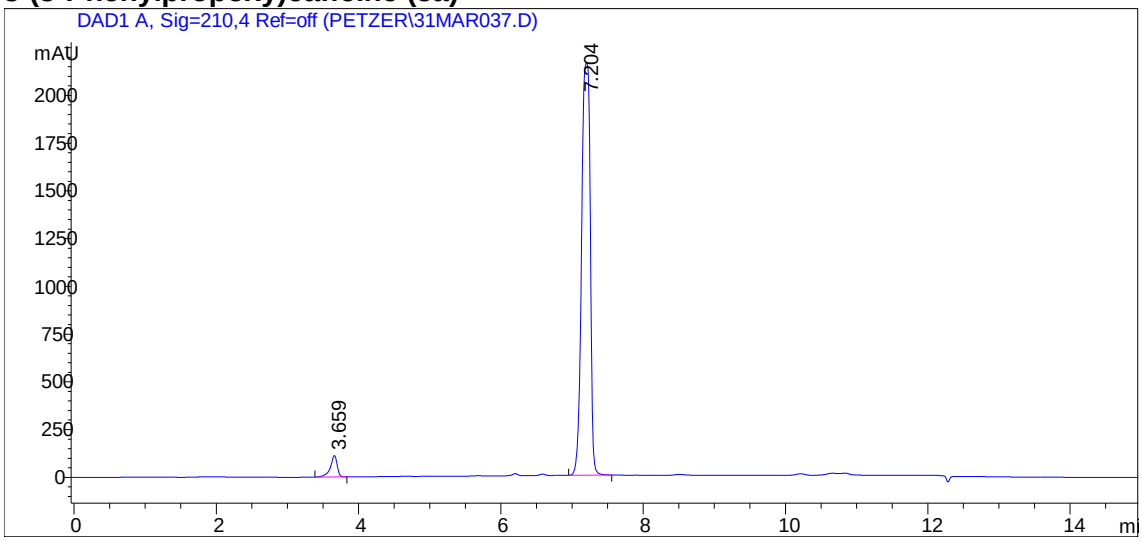

8-(3-Phenylethoxy)caffeine (5b)

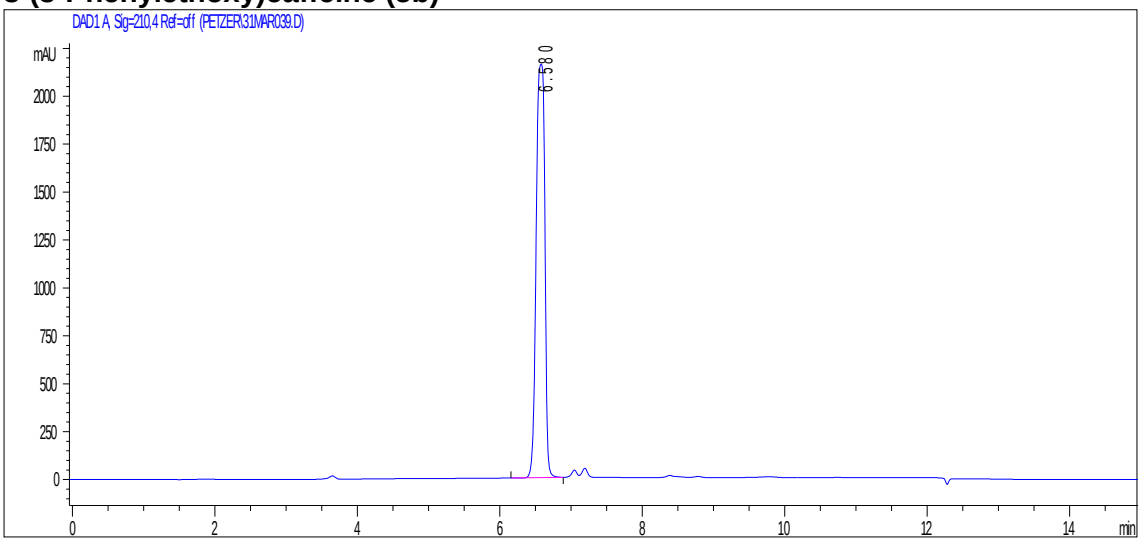

8-Phenoxycaffeine (5c)

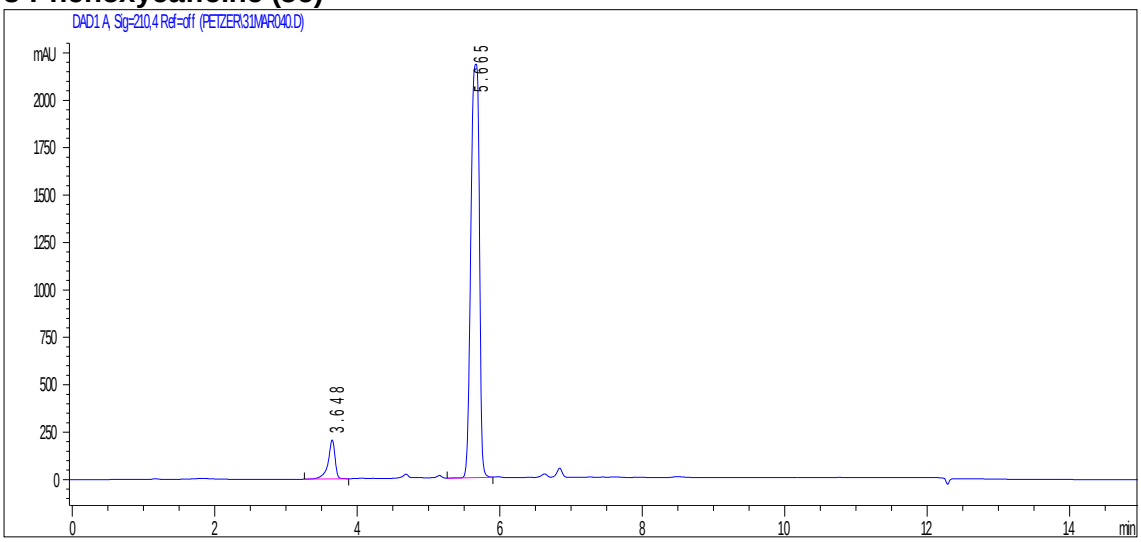

8-(4-Chlorobenzyloxy)caffeine (5d)

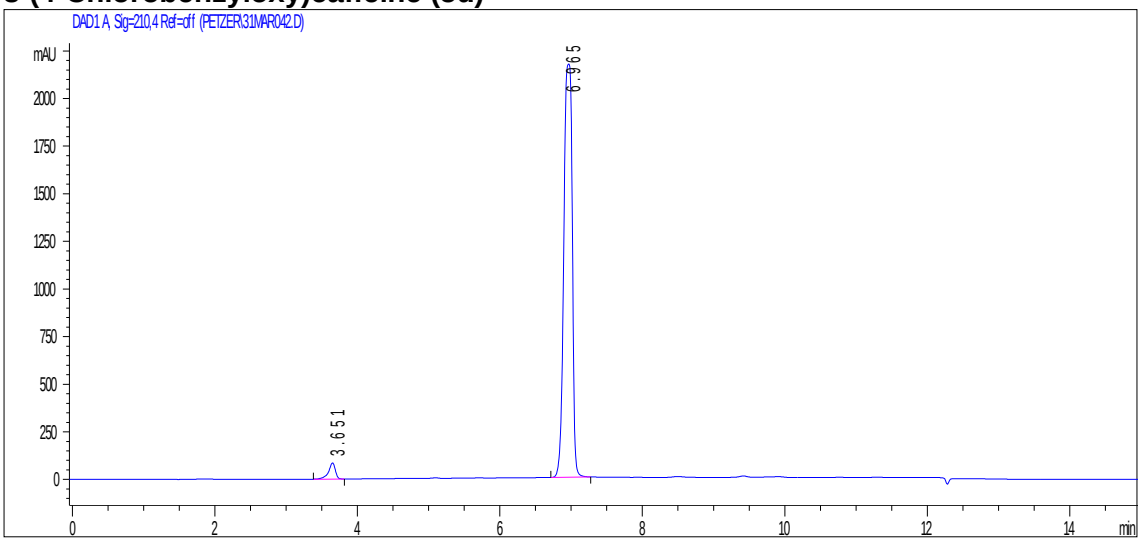

8-(4-Bromobenzyloxy)caffeine (5e)

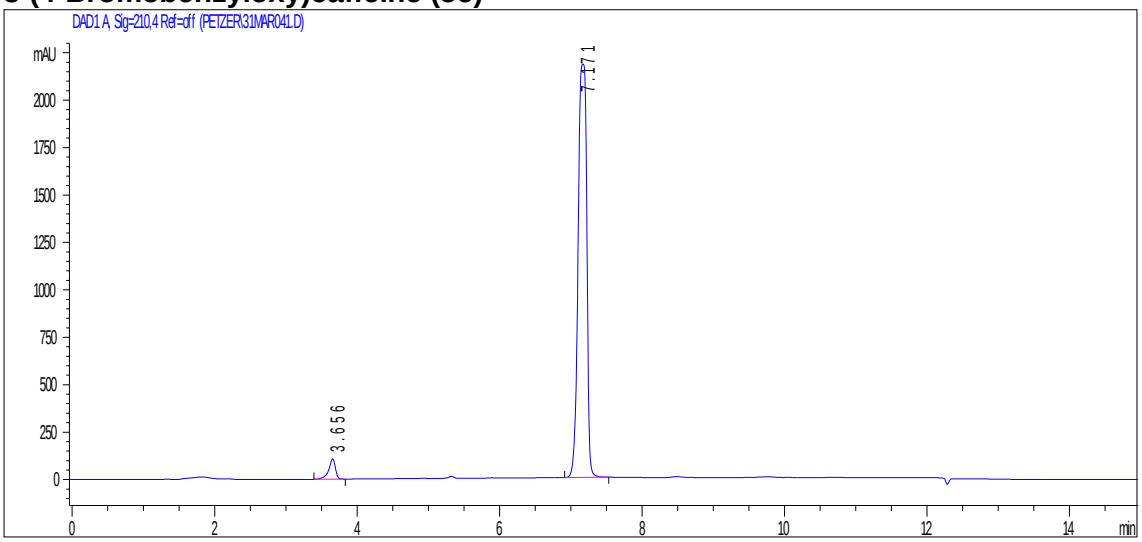

8-(Cyclohex-3-en-1-ylmethoxy)caffeine (5f)

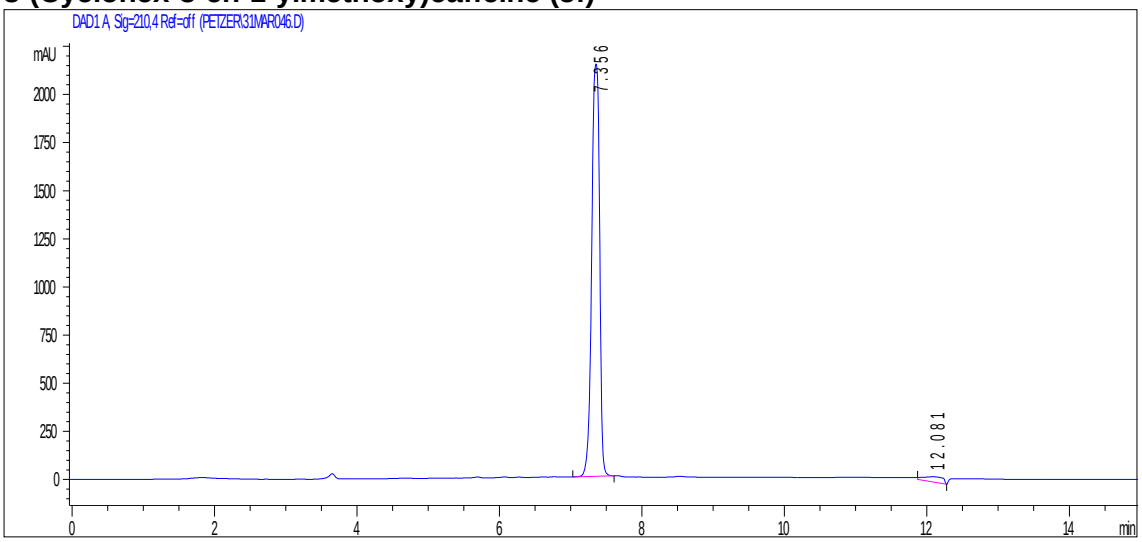

8-Cyclohexylmethoxycaffeine (5g)

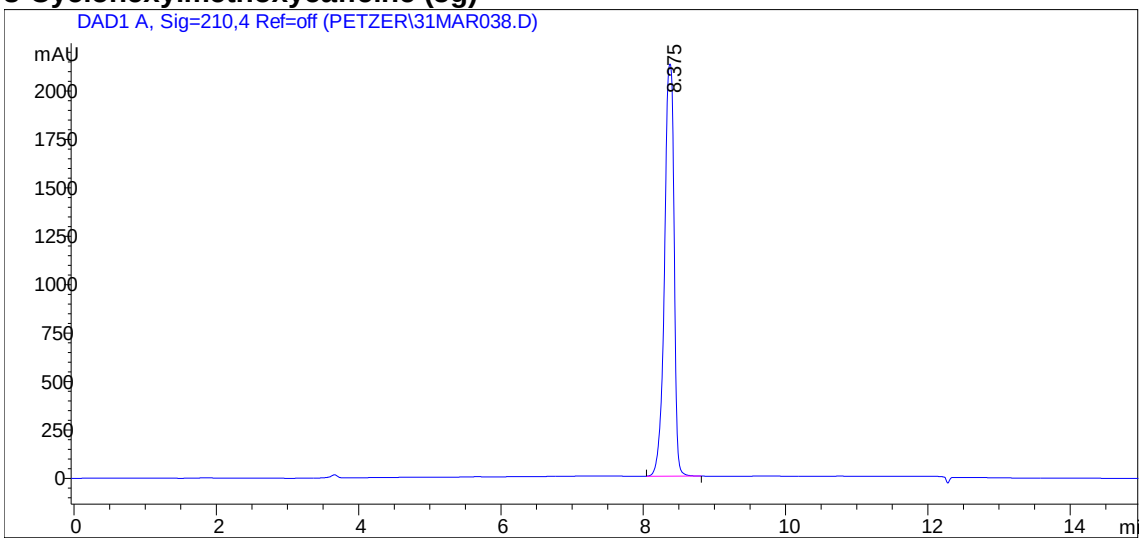

8-Cyclopentylmethoxycaffeine (5h)

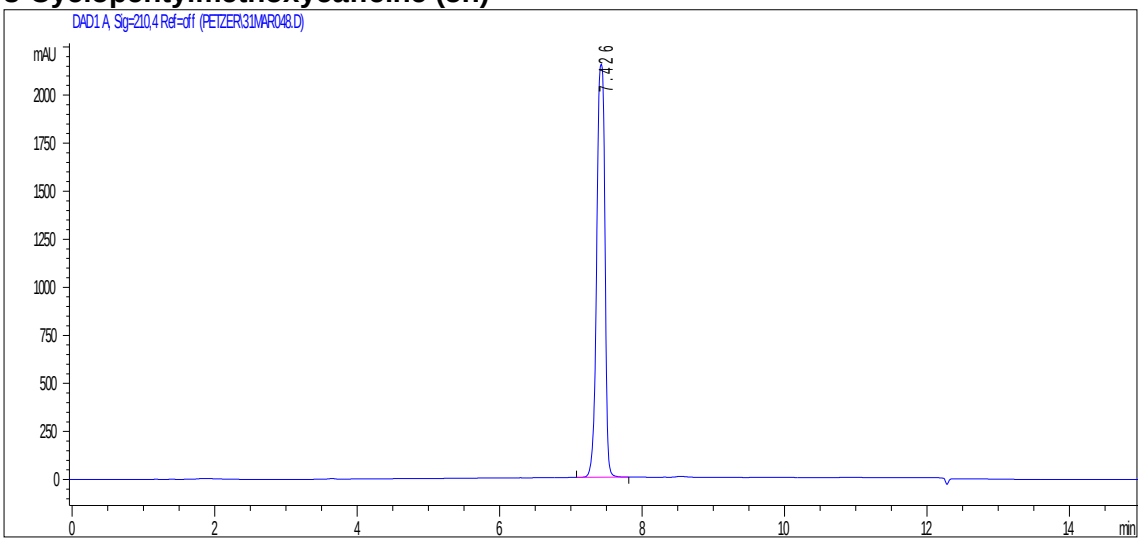

8-(2-Phenoxyethoxy)caffeine (5i)

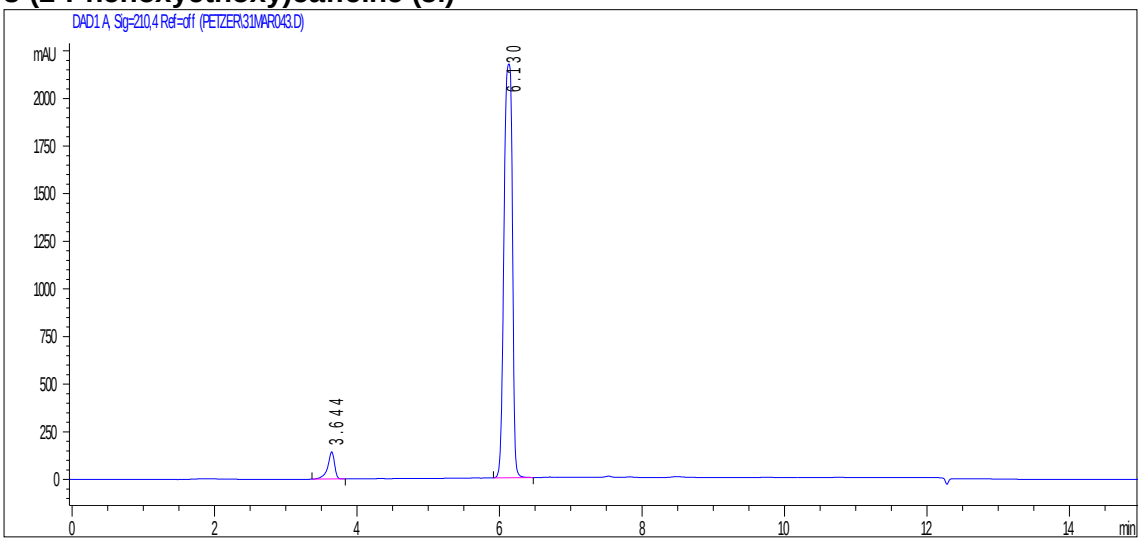

8-[2-(Benzyloxy)ethoxy]caffeine (5j)

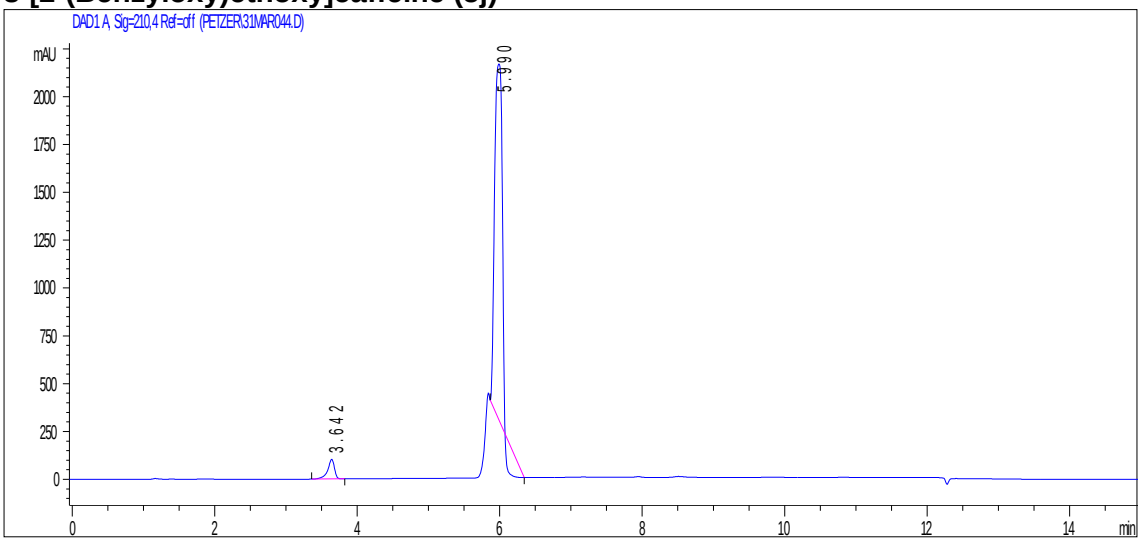

8-[(5-Methylhexyl)oxy]caffeine (5k)

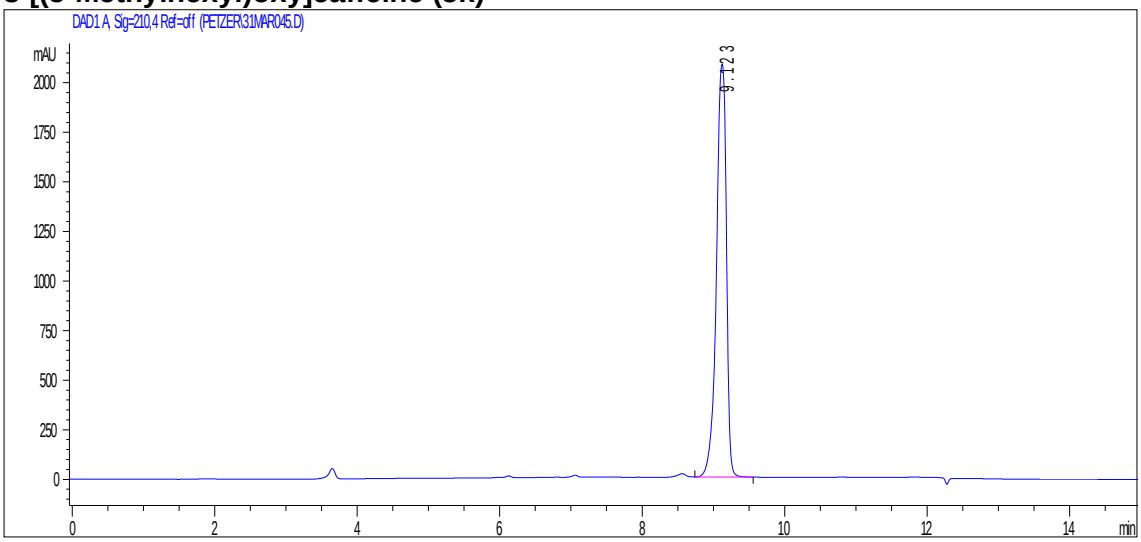

8-(3-Methylbutoxy)caffeine (5l)

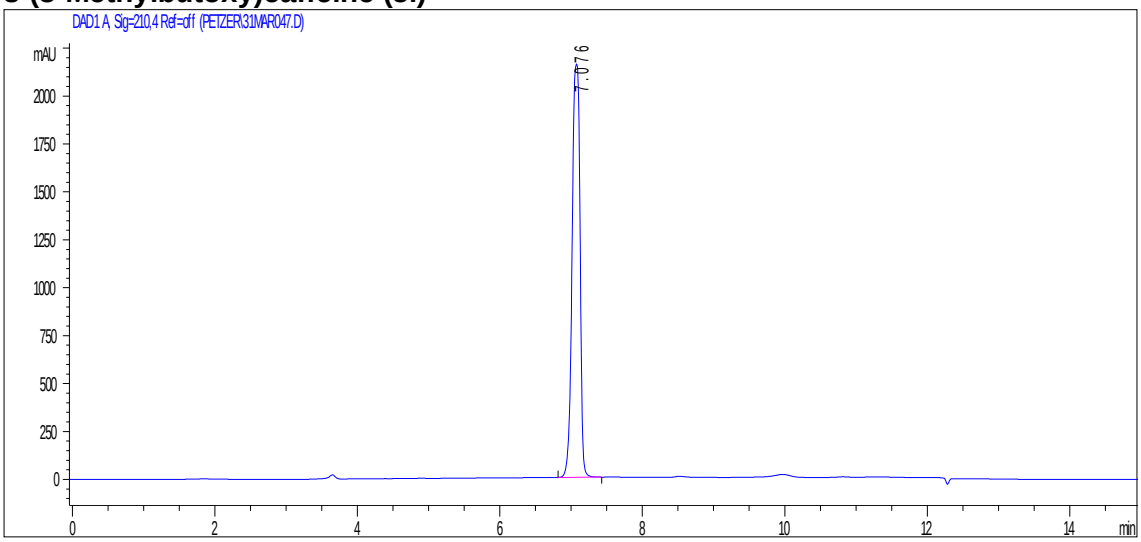

8-[2-(4-Chlorophenoxy)ethoxy]caffeine (5m)

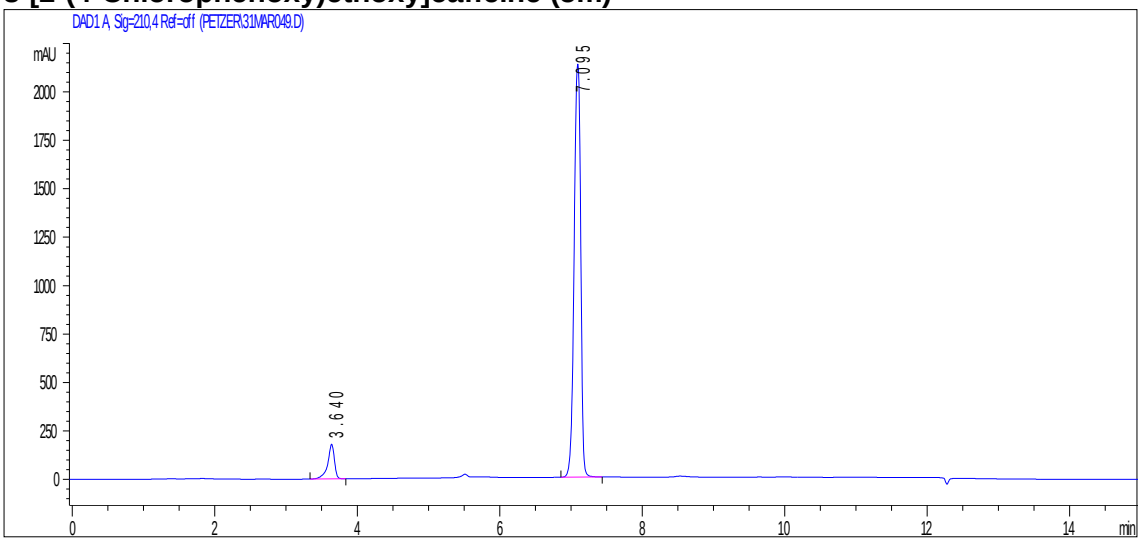

8-[2-(4-Bromophenoxy)ethoxy]caffeine (5n)

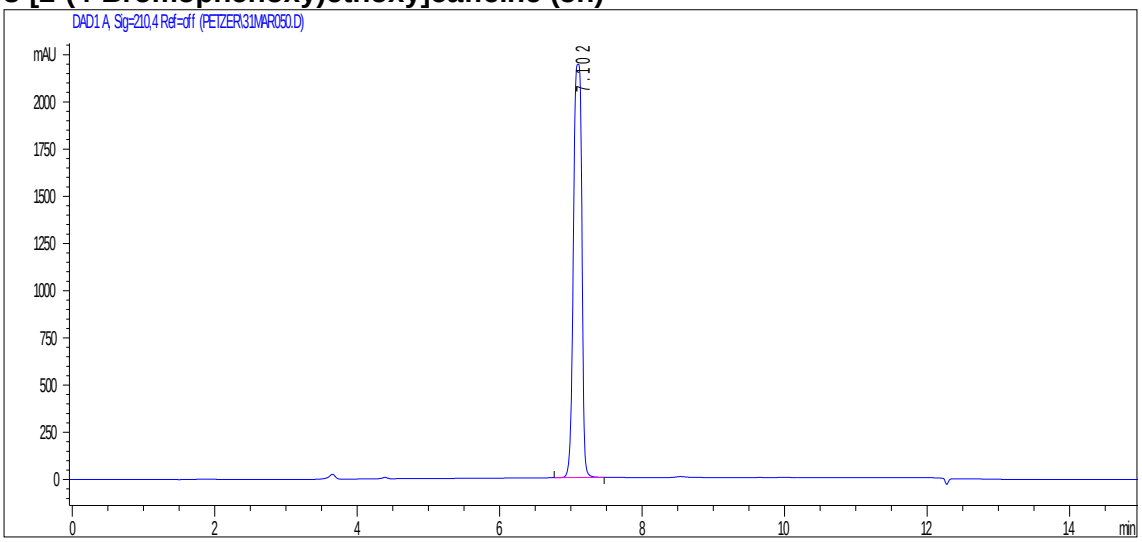

S2: ^{1}H NMR and ^{13}C NMR spectra of the following new/unknown compounds

Proton (^{1}H) and carbon (^{13}C) NMR spectra were recorded in $CDCl_3$ on a Bruker Avance III 600 spectrometer at frequencies of 600 MHz and 150 MHZ, respectively.

8-(3-Phenylpropoxy)caffeine (5a)

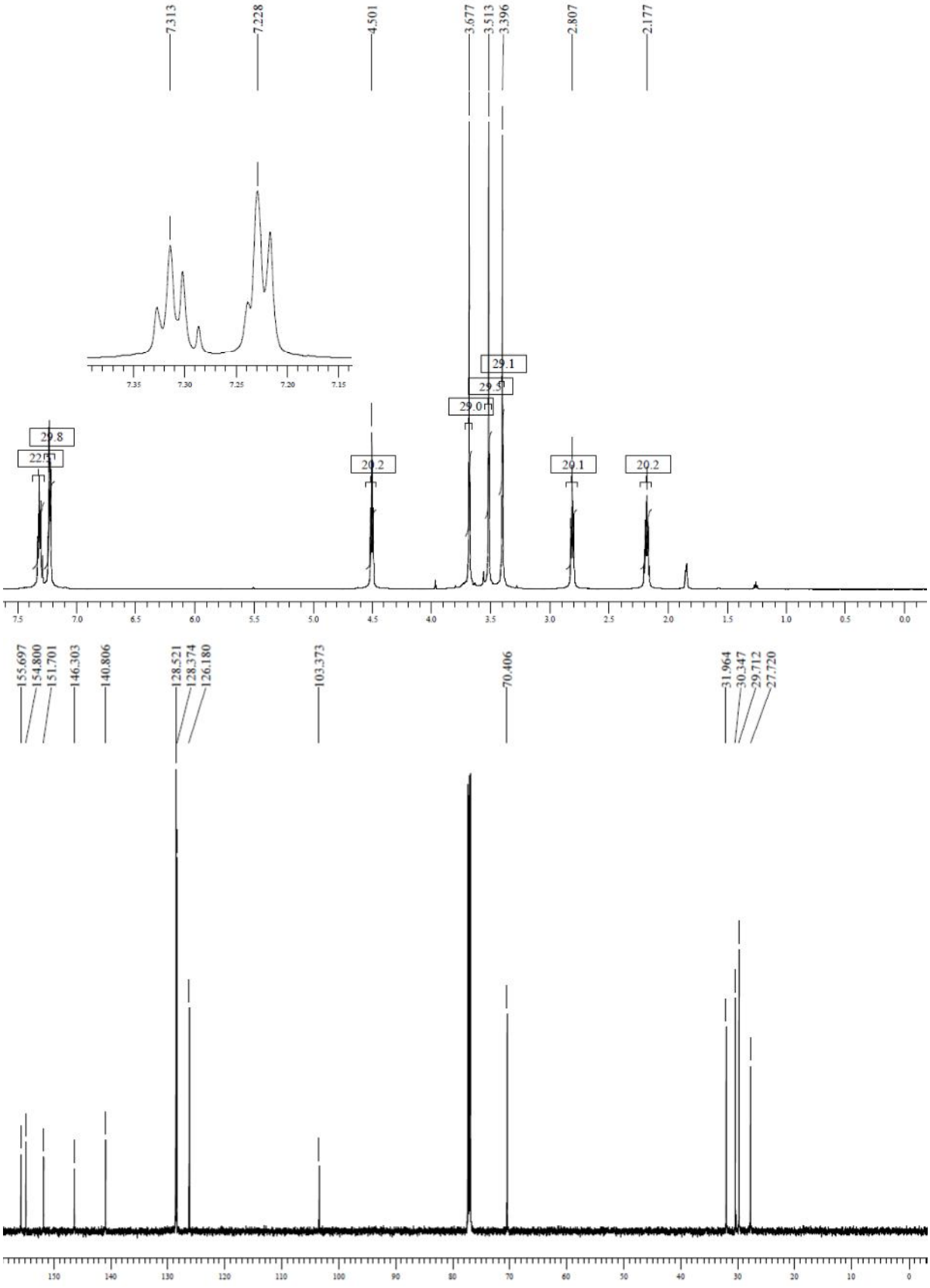

8-(3-Phenylethoxy)caffeine (5b)

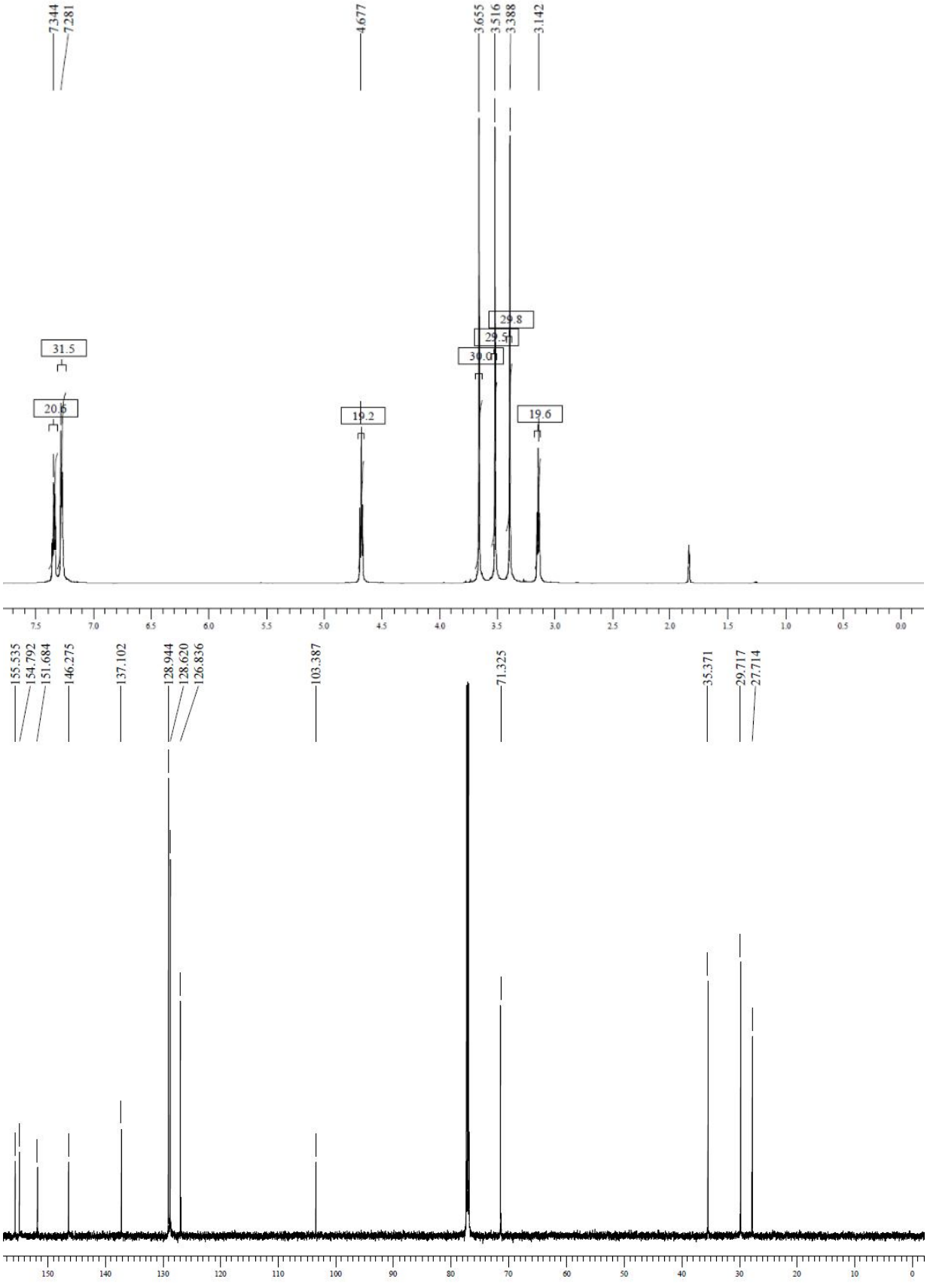

8-Phenoxycaffeine (5c)

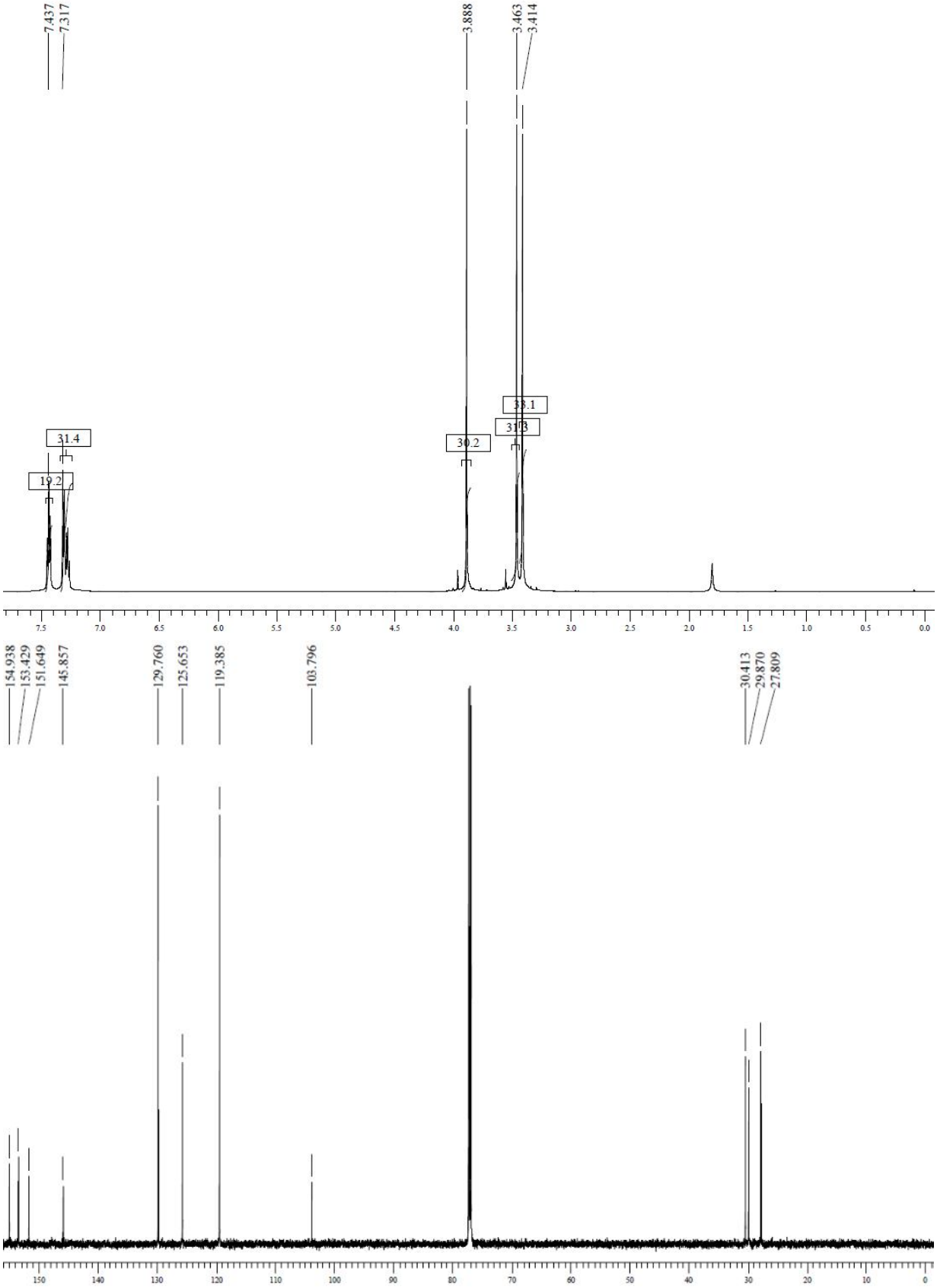

8-(4-Chlorobenzyloxy)caffeine (5d)

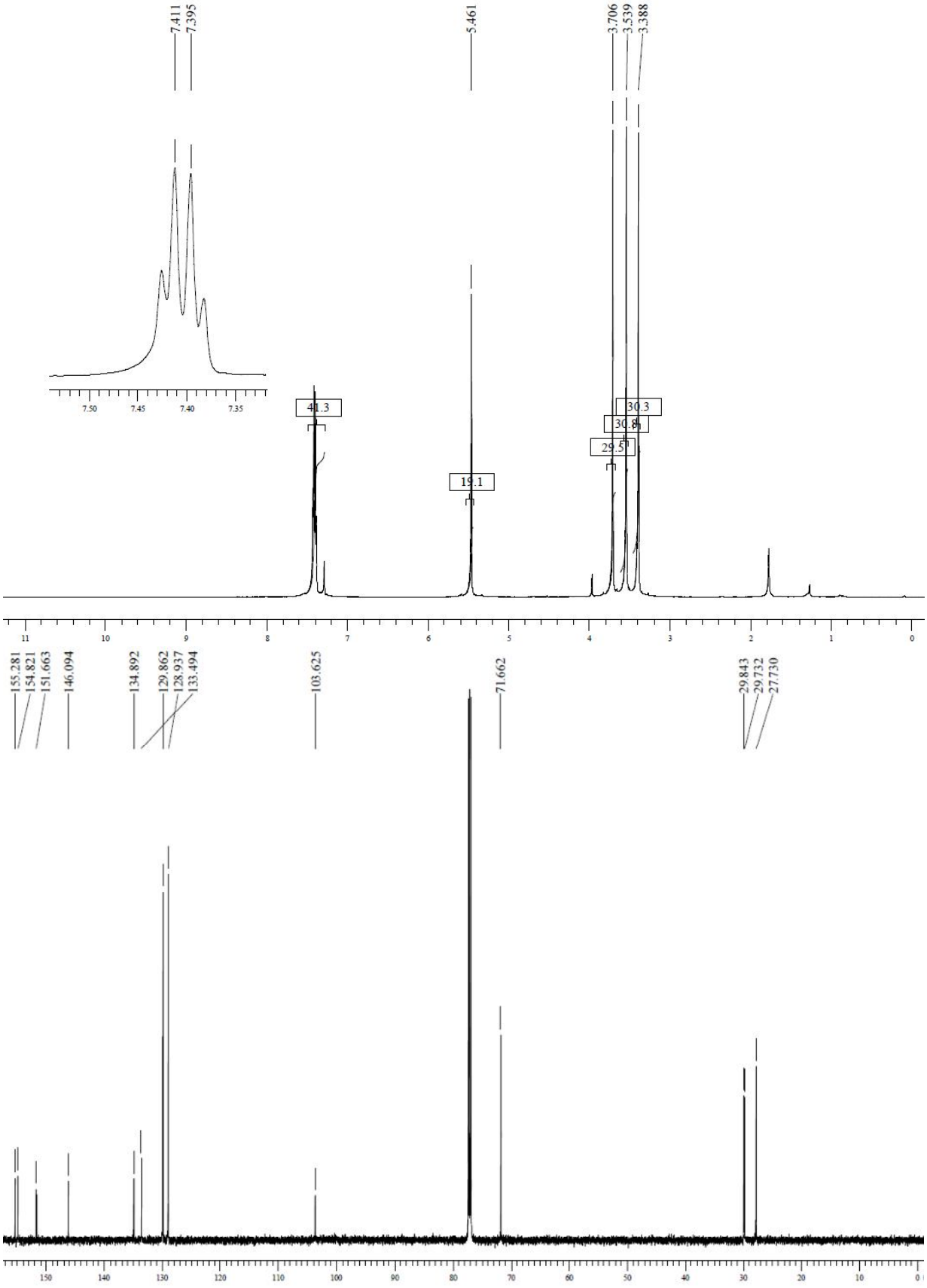

8-(4-Bromobenzyloxy)caffeine (5e)

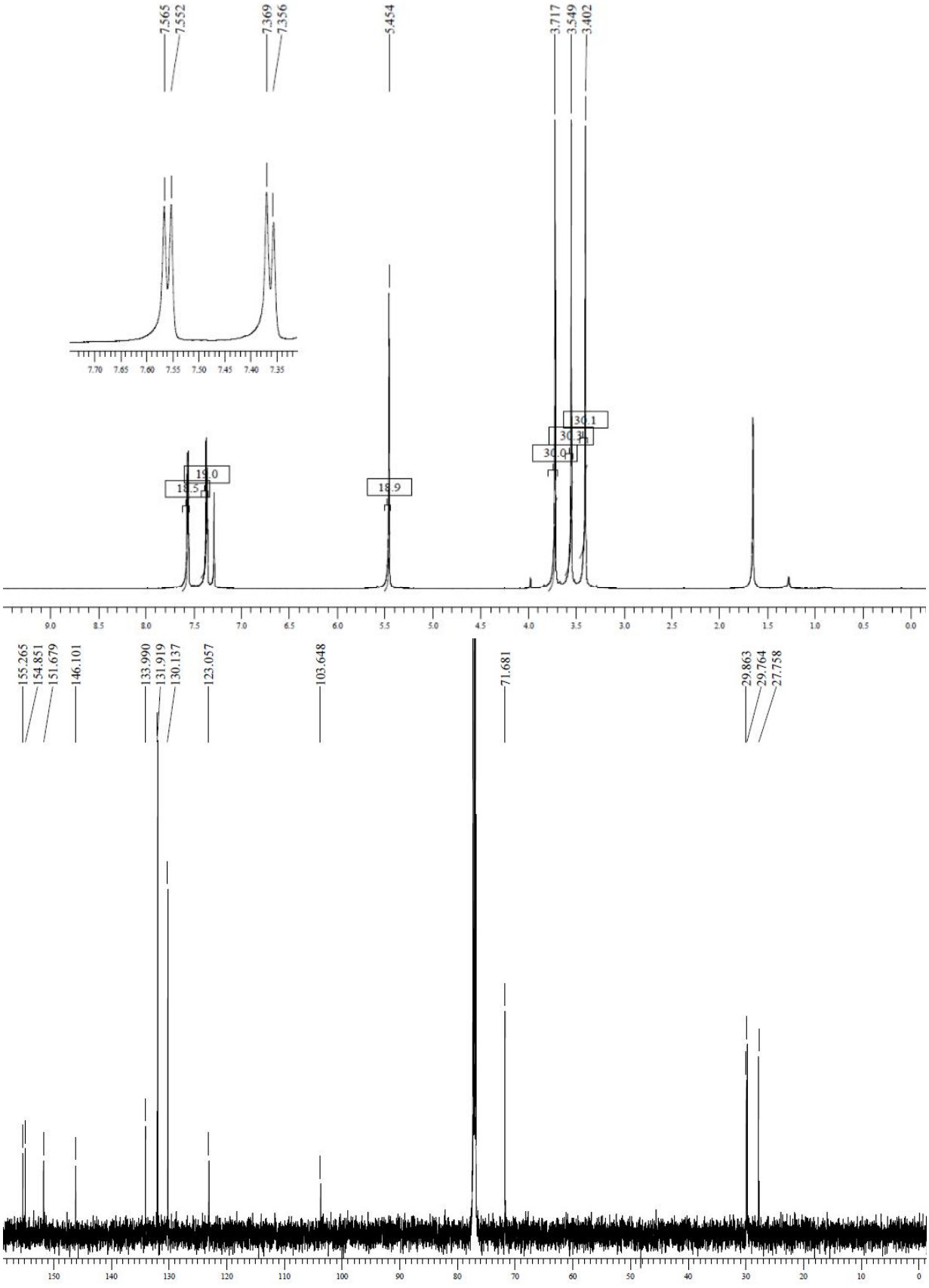

8-(Cyclohex-3-en-1-ylmethoxy)caffeine (5f)

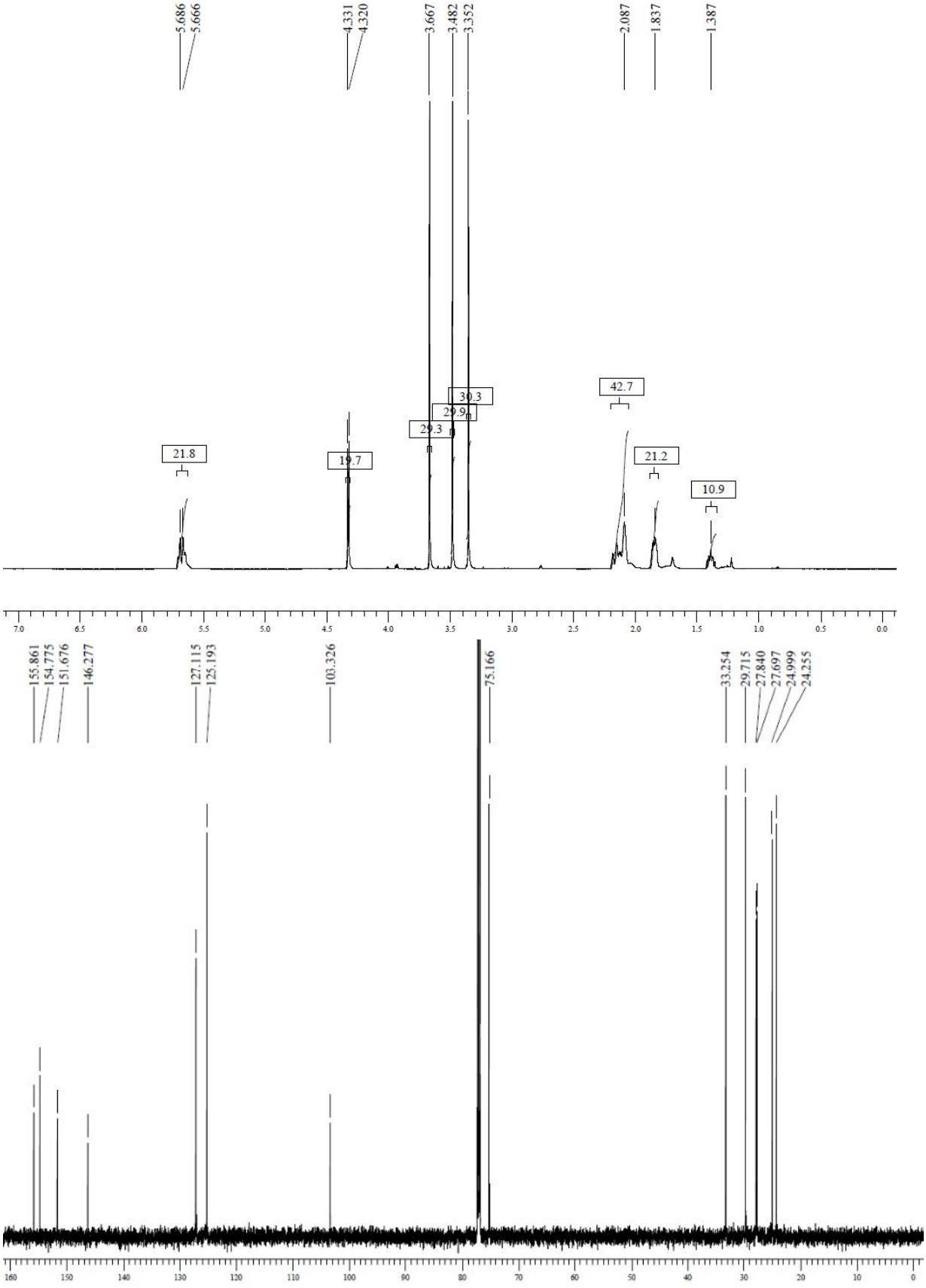

8-Cyclohexylmethoxycaffeine (5g)

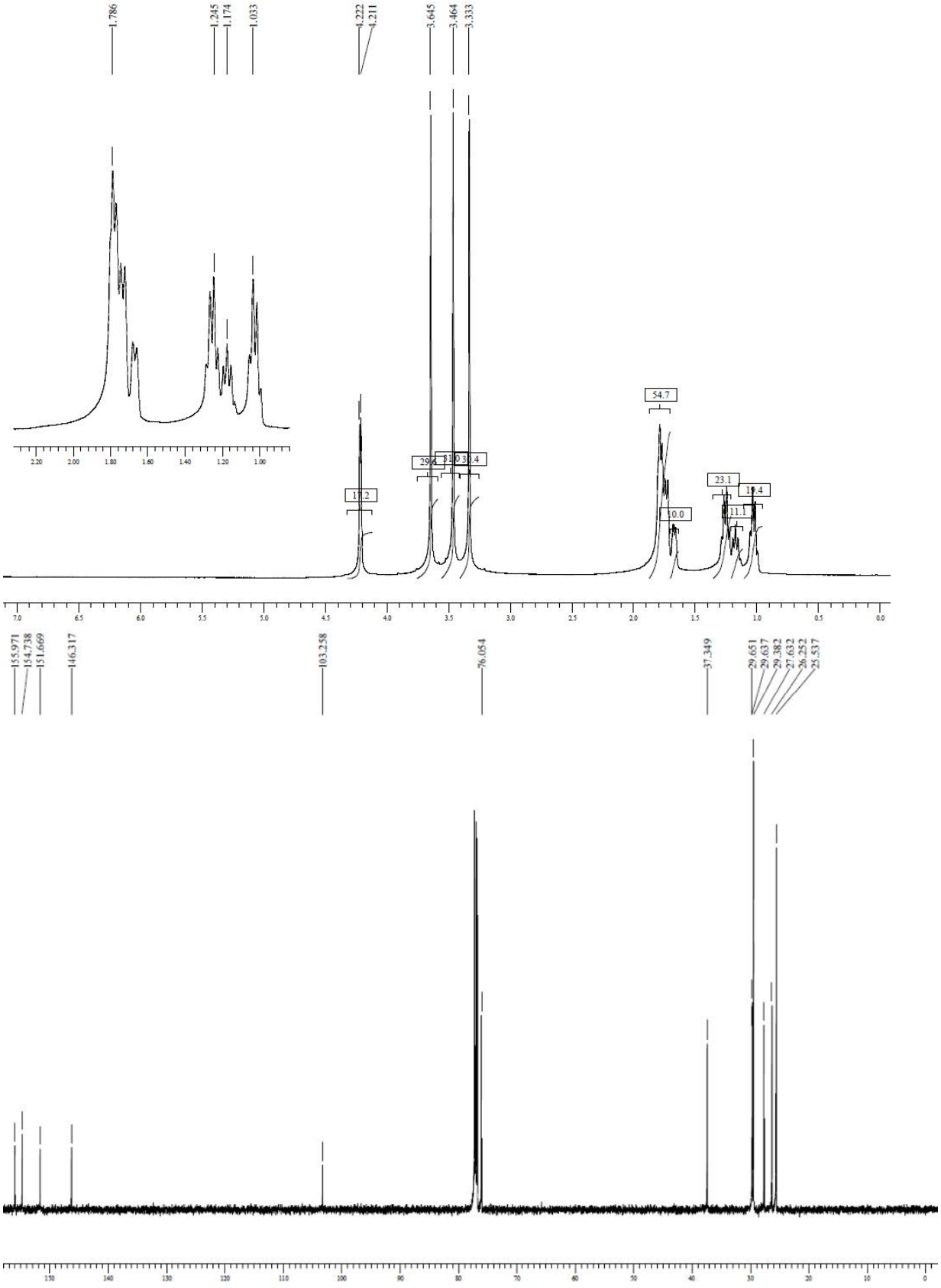

8-Cyclopentylmethoxycaffeine (5h)

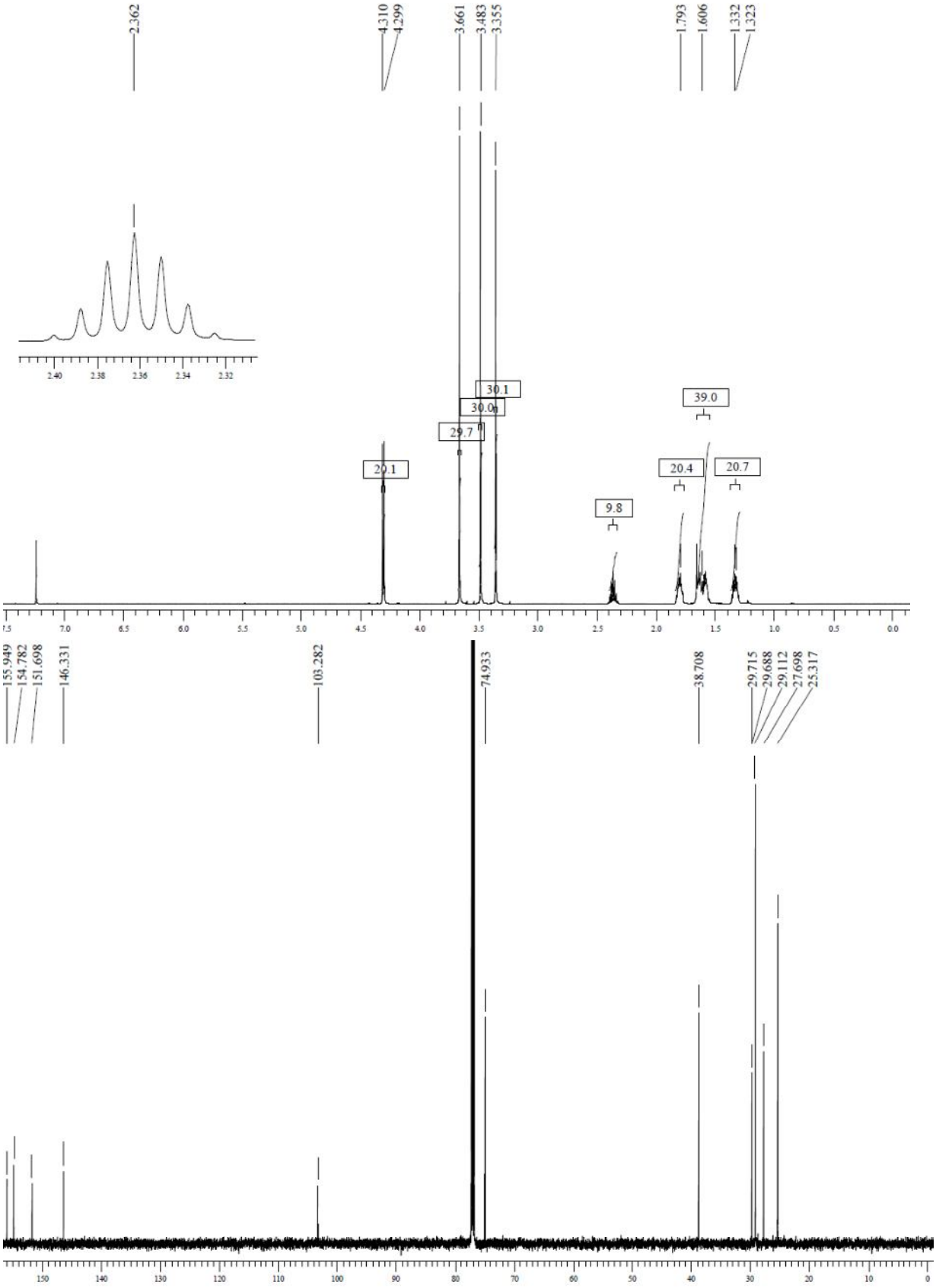

8-(2-Phenoxyethoxy)caffeine (5i)

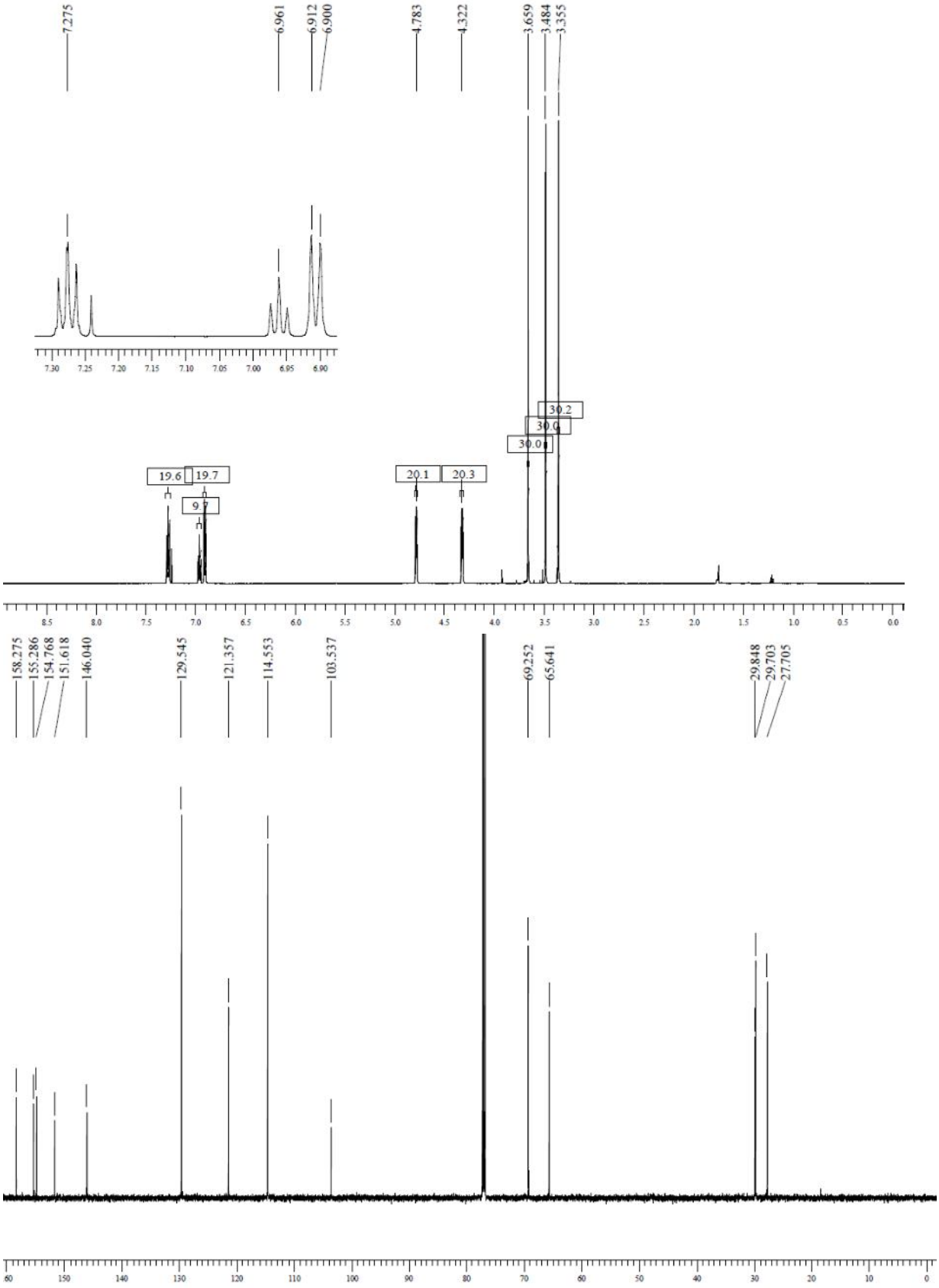

8-[2-(Benzyloxy)ethoxy]caffeine (5j)

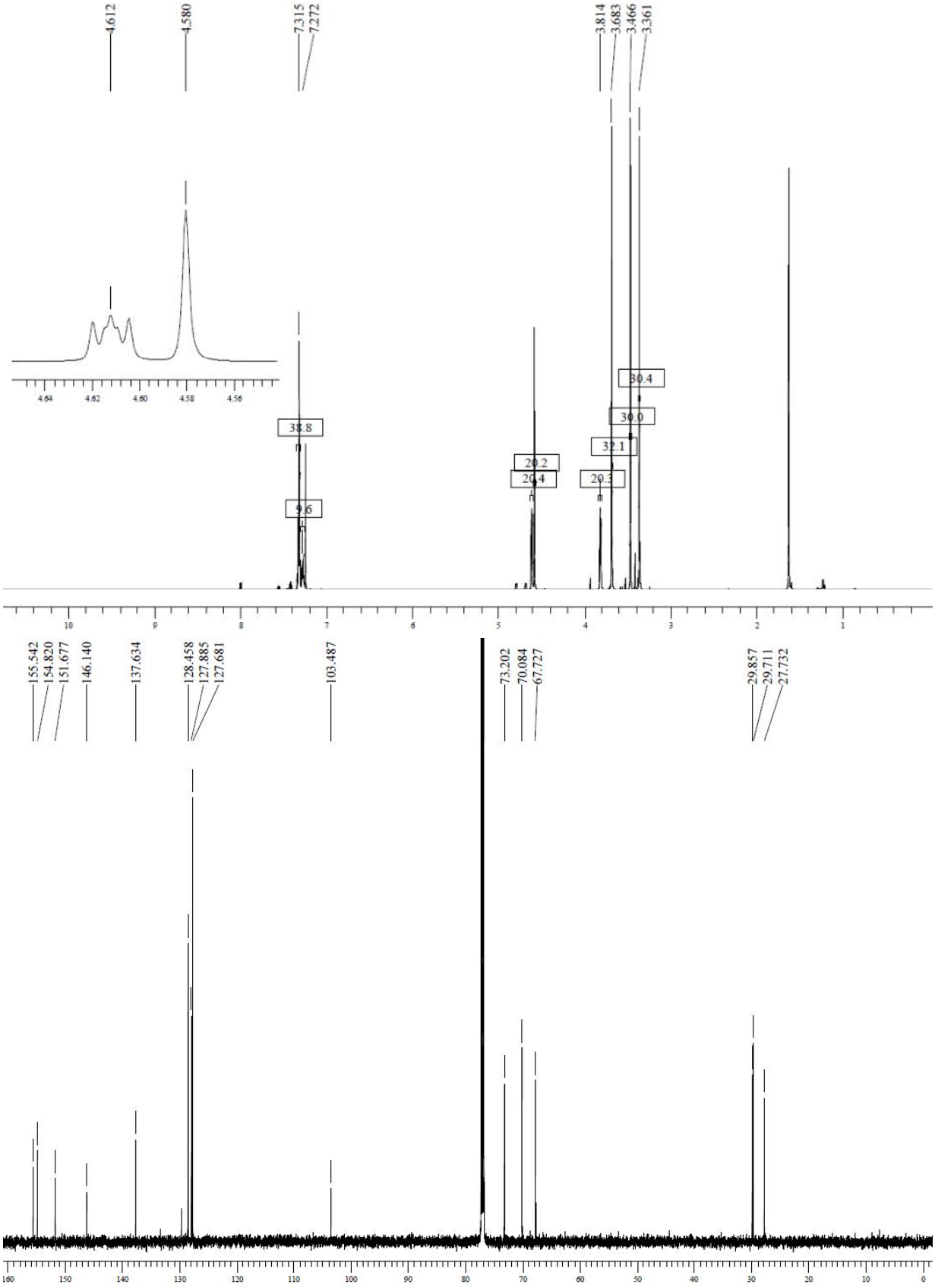

8-[(5-Methylhexyl)oxy]caffeine (5k)

8-(3-Methylbutoxy)caffeine (5l)

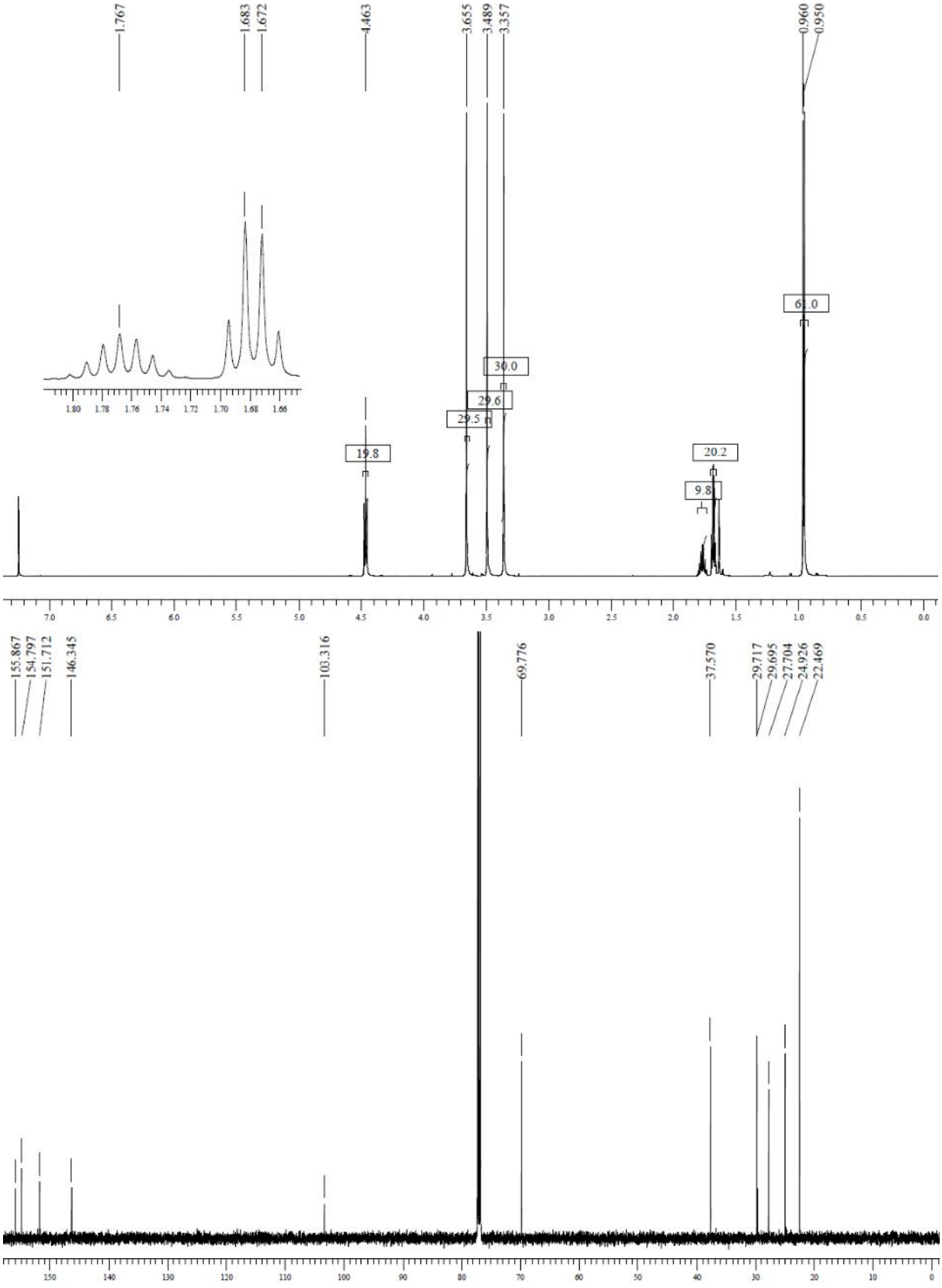

8-[2-(4-Chlorophenoxy)ethoxy]caffeine (5m)

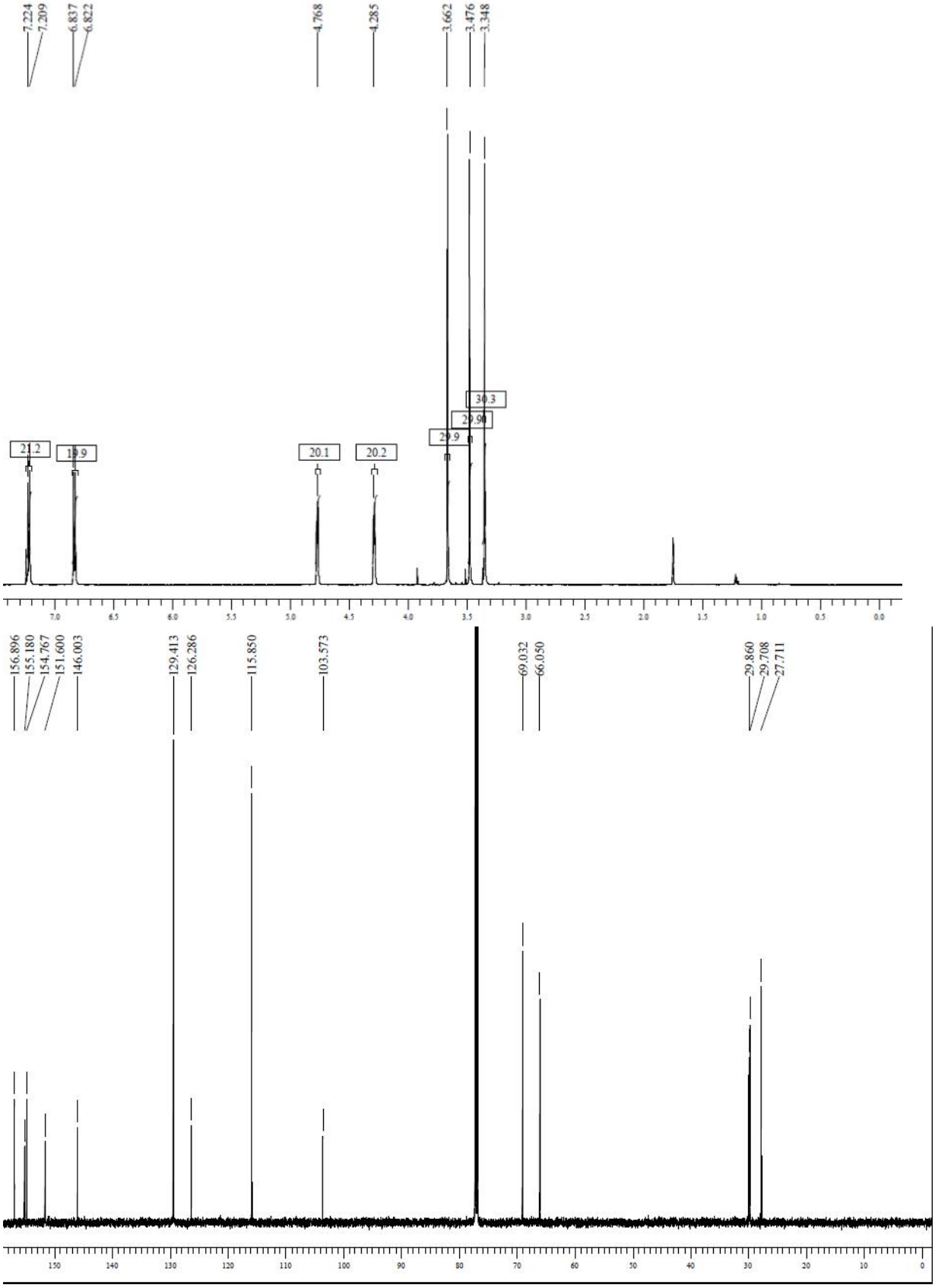

8-[2-(4-Bromophenoxy)ethoxy]caffeine (5n)